

**Probabilistic Seismic Hazard Analysis For  
Quetta City, Pakistan**



*by*

*Shafiq Ur Rehman, Najeeb Ahmed Amir, Conrad Lindholm*

*and*

*Zahid Rafi*

**Pakistan Meteorological Department**

**and**

**NORSAR**, Norway

**Technical Report No. PMD-16/2012**  
**January, 2012**

# Table of Contents

<b>Preface</b> .....	<b>5</b>
<b>Summary</b> .....	<b>6</b>
<b>1 Introduction</b> .....	<b>7</b>
<b>2 Technical approach</b> .....	<b>9</b>
2.1 Design codes and construction details .....	9
2.2 Methodology of probabilistic seismic hazard analysis .....	11
2.3 Probabilistic seismic hazard analysis .....	13
2.3.1 Theoretical framework .....	13
2.3.2 The earthquake recurrence model.....	14
<b>3 Geologic and seismotectonic setting</b> .....	<b>15</b>
3.1 Mode of faulting around Quetta.....	16
<b>4 Earlier seismic hazard and zoning results</b> .....	<b>17</b>
<b>5 Assessment of earthquake potentials</b> .....	<b>18</b>
5.1 The largest earthquakes within the greater area.....	18
5.2 Earthquake catalogues .....	19
5.2.1 Historical earthquakes .....	19
5.3 Geographical distribution of earthquake databases .....	21
<b>6 Seismotectonic zonation and quantification</b> .....	<b>22</b>
6.1 Magnitude conversions .....	22
6.1.1 Some manual magnitude assessments .....	24
6.2 Completeness, aftershocks and magnitude-frequency relation.....	24
6.2.1 Aftershocks.....	24
6.2.2 Completeness.....	24
6.3 Seismic zonation .....	27
6.3.1 The local faults included in the hazard model .....	28
6.4 Model parameters.....	30
6.4.1 Zonation and distribution of activity .....	33
6.5 Fault modeling .....	33
<b>7 Ground-motion models</b> .....	<b>34</b>
7.1 General review of models .....	35
7.2 Considered models.....	35
7.2.1 Sigma ( $\sigma$ ) values .....	37
<b>8 The computational model</b> .....	<b>37</b>
<b>9 Seismic hazard and loading results</b> .....	<b>39</b>
<b>10 References</b> .....	<b>41</b>
<b>11 Glossary</b> .....	<b>44</b>

**Illustration on front cover: Quetta at night seen from south**

## Preface

Losses from disasters caused by earthquakes will continue to increase unless there is a shift toward proactive solution and measurements. One solution is due recognition of reality that risk and vulnerability are indeed cross cutting concerns relating to economic and humanitarian sectors, with disaster reduction. The increasing pressure of growing urban population is a key consideration in the planning and implementation of disaster reduction initiatives. This research report is the contribution to the disaster risk reduction initiatives. It is fact that many cities of Pakistan are situated in the earthquake prone areas and large/small size cities are expanding in population and moving toward high hazard areas which make them increasingly risky for their residents wherein the Quetta city is one of them.

The study of seismic hazard contributes directly to sustainable development and prevents the loss of lives and infrastructure caused by earthquakes. This report is the part of hazard study carried out for Pakistan under Institutional Co-operation program (Pak-3004, Phase-II) between Pakistan Meteorological Department and Norwegian Seismic Array (NORSAR). The funding for the present study under this program was provided by the Norwegian Ministry of Foreign Affairs through Royal Norwegian Embassy in Pakistan. This program is coordinated by Public Investment Program (PIP), Ministry of Planning and Development Division, Government of Pakistan.

The national seismic hazard study, hazard study for northern areas of Pakistan and micro hazard study for Islamabad/Rawalpindi have already completed under this program by PMD and Norwegian seismic experts. Two of them are now internationally accepted (published in the international reputed scientific Journals which have high impact factor). Quetta city and surrounding areas are located in active tectonic region with the history of several destructive earthquakes. The most recent was Ziarat earthquake of 29<sup>th</sup> Oct 2008 with magnitude 6.5 but the most destructive earthquake occurred in 1935. The earthquake had a magnitude of 7.7 and more than 30,000 people died from the impact. This ranks as one of the deadliest earthquakes that hit South Asia which destroyed the entire city. This urged the need of this study.

PMD and NORSAR seismic experts viz a viz M/S Zahid Rafi, Najeeb Ahmed Amir, Shafiq Ur Rehman and Dr. Conrad Lindholm carried out research work in Pakistan and Norway. This report is written in simple and easily understood language so that its material could be easily digested not only by professionals but also by students. To this end, this study will develop a framework for risk reduction of Quetta City.



**(Arif Mahmood)**  
Director General

## Summary

Quetta city is located in the most active seismic zones of Pakistan with shallow focus earthquakes, recorded very close to the city. Over the past century Quetta has been jolted by several large events. One earthquake in 1935 destroyed almost entire city and causing casualties of around 35,000 people. Over the historical time span at least nine earthquakes with intensities between VII and X have been reported around Quetta. This stipulates the need for seismic hazard analysis of Quetta city, based on probabilistic state-of-the-art methodology.

The present research comprises of the study of active tectonics of the region, with focus on updating the existing fault systems of the study area for preparation of a seismotectonic map. The data was collected from various contributing agencies to form a composite earthquake data catalogue. The seismotectonic map and catalogue was used as the basis for the Probabilistic Seismic Hazard Analysis (PSHA) relying on area and line source modeling techniques, applying the CRISIS software (Ordaz *et al.*, 2003). No well documented ground motion prediction equations exist for the Pakistan territory. Therefore we applied a relation developed from data of similar tectonic regimes (active compression). This technique was found suitable for shallow focus seismicity for different return periods and spectral ordinates.

The results of the probabilistic seismic hazard analysis of Quetta for the return period of 500 years indicate a PGA ground motion of  $4.8 \text{ m/s}^2$ . Spectral accelerations were calculated for four different sites (Quetta North, Quetta South, Quetta East and Quetta West) of Quetta city with period between 0.003s to 2.5s. The highest spectral acceleration of  $11.6 \text{ m/s}^2$  was observed at 0.20 s for Central Quetta.

## 1 Introduction

Quetta is the capital of Balochistan, and at the same time it is a trade center and commercial hub for a main trade route between Pakistan and Afghanistan (Fig.1.1). Quetta and its surroundings are among the most earthquake active areas in Pakistan. In 1935, the city was devastated by a major earthquake event documented as a magnitude  $M=8.1$  event.

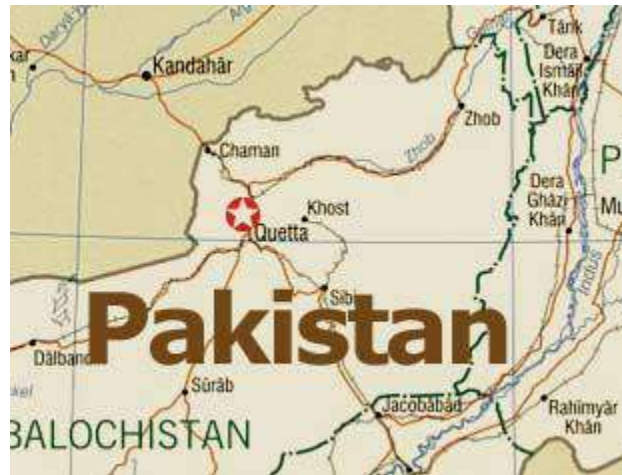


*Figure 1.1. The location of Quetta in western Pakistan bordering Afghanistan.*

In the early morning on 31 May 1935 a violent earthquake took place, which lasted for three minutes and followed by continuous aftershocks. Although there were not good enough instruments to precisely measure the magnitude of earthquake. However, estimates cite the magnitude as being a minimum of  $M_w 7.7$  and possibly as high as  $M_w 8.1$ .

The epicentre of the quake was established at 4-kilometres south-west of the town of Ali Jaan in Balochistan, that is 153-kilometres away from Quetta. The earthquake caused destruction in Quetta and almost all the towns around the city. Its tremors were felt as far as Agra in India. The largest aftershock of 5.8  $M_w$  was measured three days after the main earthquake. It did not cause any damage in Quetta but the towns of Mastung, Maguchar and Kalat were seriously affected by this aftershock. According to some authors as many as 35,000 were killed by the Quetta, 1935 earthquake (Din Muhammad 2008).

In 1931 this region already experienced two major earthquakes. The first of these near Sharigh, of  $M_w 6.8$  on 24<sup>th</sup> August 1931 followed by the Mach earthquake of  $M_w 7.3$  on 27<sup>th</sup> August 1931. Both these earthquakes caused huge damages to the property and loss of lives, though not comparable in devastation with the 1935 earthquake.



Figure 1.2. Location of Ali Jaan, assumed to be the epicenter position of the 1935 earthquake (red marker) as well as the city of Quetta (black marker) is shown.



Figure 1.3. Location of Bolan Pass is assumed to be close to one of the 1931 epicenters (Szeliga et al, 2009).

## 2 Technical approach

### 2.1 Design codes and construction details

The U.S. Army Corps of Engineers have issued a manual for Engineering and Design (U.S. Army Corps of Engineers, 1999) in which several general guidelines are included. The technical approach in that manual is generally deterministic but it contains key concepts that are applicable to the present study. The seismic assessment follows the key steps as below:

- Establishment of earthquake design criteria. In the present case this means that the definitions of Maximum Design Earthquake (MDE) and Operating Basis Earthquake (OBE) are commonly understood.
- Development of ground motion, corresponding to the MDE and OBE levels.
- Establishment of analysis procedures, i.e. procedures applied to reveal how the structure responds to the specified ground motions.
- Development of structural models.
- Prediction of earthquake response of the structure.
- Interpretation and evaluation of the results.

In the present study we will exclusively focus on the second point as above, except that we refrain from using the terms MDE or OBE. Because these terms are relevant for sensitive structures in particular, definitions of MDE and OBE as produced below gives the clear understanding:

- The Operating Basis Earthquake (OBE) is an earthquake or equivalent ground motion that can reasonably be expected to occur within the service life of the project, that is, with a 50% probability of exceedance during the service life. The associated performance requirement is that the project functions with little or no damage, and without interruption of function.
- The Maximum Design Earthquake (MDE) is the maximum earthquake or equivalent level of ground motion for which the structure is designed or evaluated. The associated performance requirement is that the project performs without catastrophic failure although severe damage or loss may be tolerated.

Ground motions for different annual exceedance probabilities are given in this study and it is the responsibility of any contractor to associate the safety levels in terms of MDE and OBE or in accordance with any other defined safety level, e.g., the national building regulations.

Peak Ground Acceleration (PGA) is the most commonly-used measure of the ground motion in seismic hazard analyses for many purposes, and it is the simplest way to characterise the damage potentials of an earthquake.

This study is entirely based on a probabilistic computation in which the expected ground motions are evaluated for various levels of exceedance probability. The various seismic provisions and guidelines reflect the seismicity level of the study area, where the expectance for the future earthquake is based on the past experience. The more detailed seismic code provisions come from regions like Japan and the United States where strong earthquakes occur frequently in regions with complex infrastructure. In such countries the seismic awareness is very high due to the combination of past experienced losses and economic strength that facilitates effective counter measures.

The seismicity of Pakistan is, characterised by many important historical and recent major earthquakes, with a steadily increasing vulnerability from its north to southwestern regions. Unfortunately, the seismic awareness in these regions is still very low.

Seismic design codes have the purpose of providing building guidelines for the reduction of both property and life losses due to the seismic events. These building design codes define standards for the seismic resistant design for the construction of new building and for the retrofit of the existing ones. Guidelines are developed on the basis of sound theoretical, physical modelling and the observed damages caused by major earthquakes. The lessons given by past earthquakes help to promote advances in the development of design methods, knowledge of materials performance and for enhancement of construction practices.

Basically, seismic code contains specifications for the seismic hazard, including soil and possible near-fault effects that should be used in seismic design of buildings in the concerned region, which in turn is based on a base shear load that the building should resist. In Europe there has been a great effort in launching a set of so-called Eurocodes (EC) which contain complete guidelines for the construction industry including the seismic provisions (EC 8, 2004). Eurocode 8 defines two goals of the anti-seismic design:

- The structure shall be designed to withstand the designed seismic action without local or general collapse.
- The structure shall be designed and constructed to withstand a seismic action (seismic load) having a higher probability of occurrence than the design seismic action.

Modern codes, notably the 1997 Uniform Building Code (ICBO, 1997) and the EC-8, 2004, are based upon the specification of base shear that depends on the seismic hazard level of the site, site effects coming from the site geology, near fault effects, weight, fundamental period, lateral forces, and the resisting system of the building. In areas of high seismicity, sufficient ductile detailing to accommodate the inelastic demand (Bachman and Bonneville, 2000) is needed.

The objective of this study is to provide the seismic actions at various annual exceedance probability levels. The building constructors/designers must choose an appropriate risk level/exceedance probability level for the structure for which the design ground motion is associated.

The selection of the appropriate risk level is essentially a question of consequences of a failure. The risk level is most often specified either as annual exceedance probability or as exceedance probability during the expected lifetime of the structure. The discussion of risk levels is supported by the following correlation between return period  $T_R$  and lifetime  $T$ , where  $P$  is annual probability of exceedance (see also Fig. 2.1):

$$T_R = \frac{-T}{\ln(1 - P(Z > z))}$$

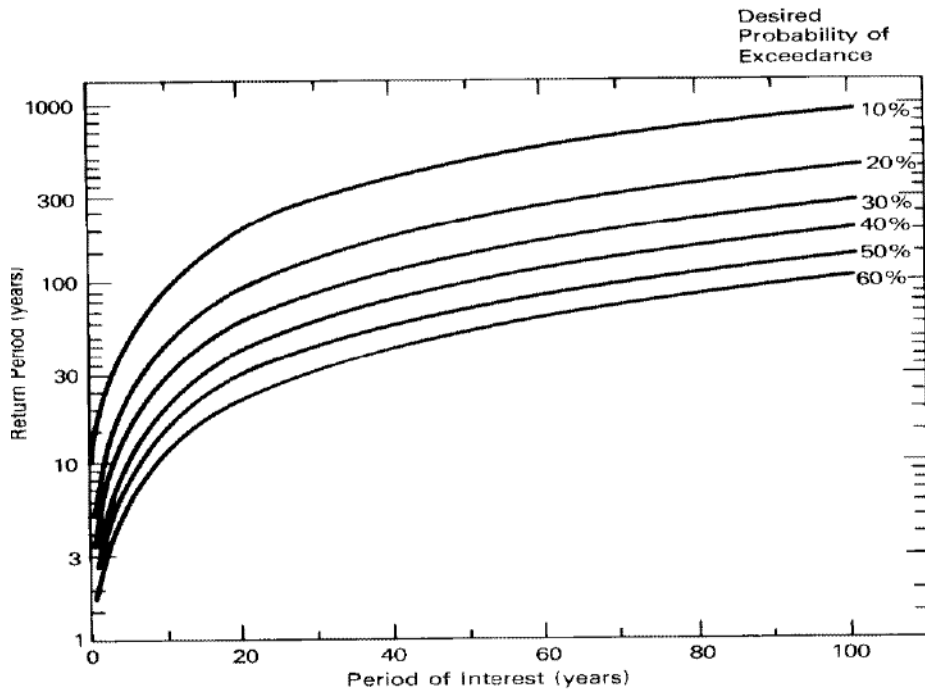


Figure 2.1. Relationship between return periods (inverse of annual exceedance probability), period of interest and desired probability of exceedance during the period of interest (according to Reiter, 1990).

For example, if the expected lifetime of a structure is  $T = 200$  years, and a 95% non-exceedance probability (5% exceedance probability,  $P = 0.05$ ) is required, then this safety requirement corresponds to a return period of  $T_R = 3900$  years, or an equivalent of  $3 \times 10^{-4}$  annual exceedance probability. The curves for various lifetime structures and the corresponding return periods are shown in Fig. 2.1.

## 2.2 Methodology of probabilistic seismic hazard analysis

It is well known that uncertainties are essential in the definition of all elements that go into seismic hazard analysis in particular since the uncertainties often drive the results, and increasingly so for low-exceedance probabilities. It can sometimes lead to difficult choices for decision makers. Rational solutions to dilemmas posed by uncertainty can be based on the utilization of some form of probabilistic seismic hazard analysis. In contrast to the typical deterministic analysis, which (in its simplest form) makes use of discrete single-valued events or models to arrive at the required description of earthquakes hazard. The probabilistic analysis allows the use of multi-valued or continuous model parameters. Of most importance, the probability of different magnitude or intensity earthquakes occurring is included in the analysis. Another advantage of probabilistic seismic hazard analysis is that it results in an estimate of the likelihood of earthquake ground motions or other damage measures occurring at the location of interest. It allows for the more sophisticated incorporation of seismic hazard into seismic risk estimates. Probabilistic seismic hazard estimates can be expanded to define seismic risk.

The methodology used in most Probabilistic Seismic Hazard Analysis (PSHA) was first defined by Cornell (1968). There are four basic steps for assessment of PSHA:

**Step 1** is the definition of earthquake sources. Sources may range from small faults to large seismotectonic provinces with uniform seismicity.

**Step 2** is the definition of seismicity recurrence characteristic for the sources, where each source is described by an earthquake probability distribution, or recurrence relationship. A recurrence relationship indicates the chance of an earthquake of a given size to occur anywhere inside the source during a specified period of time. A maximum or upper bound earthquake is chosen for each source, which represents the maximum event to be considered, because these earthquakes are assumed to occur anywhere within the earthquake source, distances from all possible location within that source to the site must be considered.

**Step 3** is the estimation of the earthquake's ground shaking effect. The range of earthquake sizes requires a family of earthquake attenuation or ground motion curves, each relating to a ground motion parameter (e.g. peak ground acceleration), as function of distance for an earthquake of a given size.

**Step 4** is the determination of the hazard at the site, which is substantially dissimilar from the procedure used in arriving at the deterministic hazard. In this case the effects of all the earthquakes of different magnitudes occurring at different locations and in different earthquake sources at different probabilities of occurrence are integrated into one curve that shows the probability of exceeding different levels of ground motion (such as peak acceleration) at the site during a specified period of time. With some assumptions it can be written as:

$$E(Z) = \sum_{i=1}^N \alpha_i \int_{m_o}^{m_u} \int_{r=0}^{r=} f_i(m) f_r(r) P(Z > z | m, r) dr dm$$

where  $E(Z)$  is the expected number of exceedances of ground motion level  $z$  during a specified time period  $t$ ,  $\alpha_i$  is the mean rate of occurrence of earthquakes between lower and upper bound magnitudes ( $m_o$  and  $m_u$ ),  $f_i(m)$  is the probability density distribution of magnitude within the source  $I$ ,  $f_i(r)$  is the probability density distribution of epicentral distance between the various locations within source  $I$  and the site for which the hazard is being estimated,  $P(Z > z | m, r)$  is the probability that a given earthquake of magnitude  $m$  and epicentral distance  $r$  will exceed ground motion level  $z$ .

While carrying out the probabilistic seismic hazard analysis it is usually assumed that earthquakes occurrences are of Poisson distribution and hence have no memory. It implies that each earthquake occurs independently of any other earthquake.

One of the most important recent developments within PSHA is seismic source modelling. Originally, seismic sources were crudely represented as line sources (Cornell, 1968) and later area zones, which could be narrowed to represent the surface outcrop of faults as in McGuire's (1976) computer program EQRISK. An improved scheme, which included the effects of fault rupture, was proposed by Der Kiureghian and Ang (1977), and in a modified form was implemented by McGuire (1978) in his fault modelling program FRISK, written as a supplement to his earlier and very popular EQRISK area source program.

While the standard practice for a long time was to present the results of seismic hazard analyses in terms of a single best-estimate hazard curve, the growing awareness of the importance of parametric variability and the trend to consult expert opinion in matters of scientific doubt, led to the formulation of Bayesian models of hazard analysis (Mortgat and Shah, 1979) which seek to quantify uncertainty in parameter assignment in probabilistic terms.

In the present work we have applied the CRISIS computer code for seismic hazard assessment (Ordaz *et al.*, 2003). The code accommodates uncertainty in a number of the seismicity model parameters, and has a user-friendly interface. It accepts polygon-dipping areas as well as fault sources, and also facilitates characteristic earthquake recurrence models.

## 2.3 Probabilistic seismic hazard analysis

### 2.3.1 Theoretical framework

The model for the occurrence of ground motions at a specific site in excess of a specified level is assumed to be that of a Poisson process. This follows if the occurrence of earthquakes is a Poisson process, and the probability of an event will produce site ground motions in excess to a specified levels is independent of the occurrence of other events. The probability that a ground motion level is exceeded at a site in unit time is thus expressed as:

$$P(Z > z) = 1 - e^{-v(z)}$$

where  $v(z)$  is the mean number of events per unit time in which  $Z$  exceeds  $z$ . In the conventional method of probabilistic hazard analysis (McGuire, 1976), the region around a site is partitioned into polygons, which constitute a set of area sources. Basic differences in seismicity and geology may exist between the zones; however, it is assumed that the seismicity within each zone is sufficiently homogeneous to be treated uniformly in the computations. This assumption applies even where non-seismological criteria have been used in the zone definition, e.g., geological structures. With  $N$  seismic sources, and seismicity model parameters  $S_n$  for any source  $n$ , the mean number of events pr. unit time in which ground motion level  $z$  is exceeded can be written as:

$$v(z) = \sum_{n=1}^N v_n(z | S_n)$$

where

$$v_n(z | S_n) = \sum_{i,j} \lambda_n(M_i | S_n) \cdot P_n(r_j | M_i S_n) \cdot G_n(z | r_j M_i S_n)$$

and where  $\lambda_n(M_i | S_n)$  is the mean number of events per unit time of magnitude  $M_i$  ( $M_i \in [M_{\min}, M_{\max}]$ ) in the source  $n$  with seismicity parameters  $S_n$ . Moreover,  $P_n(z | M_i S_n)$  is the probability that a significant site–source distance is  $r_j$ , ( $r_j \in (r_{\min}, r_{\max})$ ) given an event of magnitude  $M_i$  at distance  $r_j$  in source  $n$  with seismicity parameters  $S_n$ . The expression  $G_n(z | r_j M_i S_n)$  is the probability that ground motion level  $z$  will be exceeded, given an event of magnitude  $M_i$  at distance  $r_j$  in source  $n$  with seismicity parameters  $S_n$ . The three functions  $\lambda_n(M_i | S_n)$ ,  $P_n(z | M_i S_n)$  and  $G_n(z | r_j M_i S_n)$  model the inherent stochastic uncertainty in the frequency of occurrence and location of earthquakes, in the attenuation of seismic waves.

Given that the mean number of events per unit time for which  $Z$  exceeds  $z$  is expressed for example as  $1/T_R$ , where  $T_R$  is the return period (inverse of annual exceedance probability), then the number of events in a time period  $T$  (e.g. the life time of a certain construction) for which  $Z$  exceeds  $z$  is given by  $T/T_R$  and the probability for  $Z$  exceeding  $z$  during the life time  $T$  is given by:

$$P(Z > z) = 1 - e^{-T/T_R}$$

For a life time  $T$  of 50 years and a return period  $T_R$  of 475 years (annual probability of exceedance  $0.211 \times 10^{-2}$ ) the probability for  $Z$  exceeding  $z$  becomes 0.1, corresponding to 90%

probability that size of the ground motion is not exceeded in 50 years. This is also illustrated in Fig. 2.1.

With several seismic sources, described through particular model parameters, the mean number of events per unit time in which the ground motion level  $z$  is exceeded can be expressed specifically by involving functions that model the inherent stochastic uncertainty in the frequency and location of earthquakes, and in the attenuation of the seismic waves.

### 2.3.2 The earthquake recurrence model

The recurrence rate of earthquakes is assumed to follow the cumulative Gutenberg-Richter relation:

$$\log N(M) = a - bM$$

Here  $N(M)$  is the number of events per year with magnitude greater or equal than  $M$ . This relation appears with few exceptions to hold quite well, indicating a self-similarity of earthquakes.

In seismic hazard analyses a modified and truncated version of this relation is used, involving engineering threshold magnitude  $M_{lim}$ , limiting upper bound magnitude  $M_{max}$  for the source, a slope parameter  $\beta = b \ln(10)$  that describes the relation between the number of smaller and larger earthquakes, and an activity rate parameter  $A = a(M_{lim})$  which describes the number of events on the source with magnitude equal to or greater than  $M_{lim}$ . See Fig. 2.2 for two recurrence models.

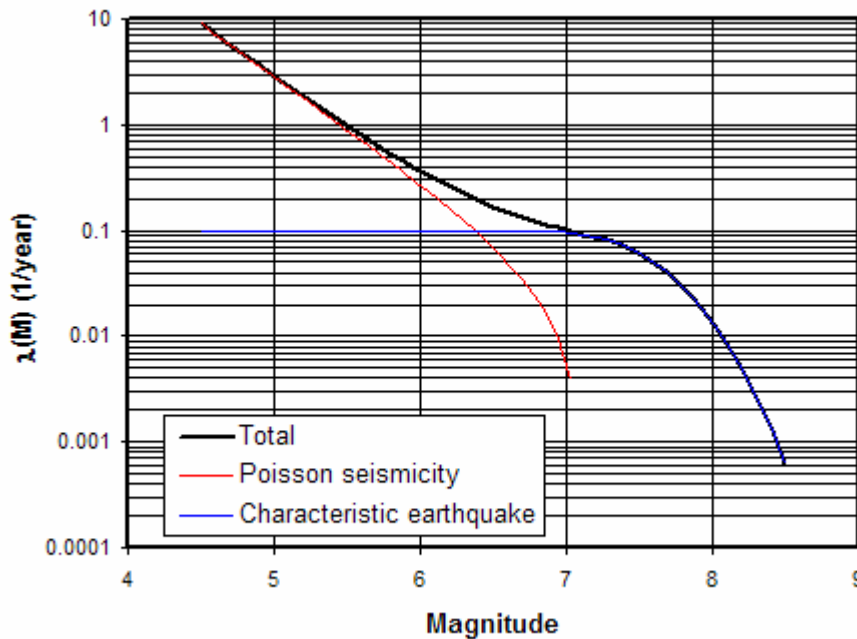


Figure 2.2. Earthquake recurrence functions. The red line indicates the truncated cumulative Gutenberg-Richter relation, while the blue line indicates the truncated characteristic recurrence model used in CRISIS (Ordaz et al., 2003).

The activity rate parameter is liable to vary substantially from one seismic source to another while the  $b$ -value is expected to be regionally stable, with variations less than the uncertainty limits. Faults, which may be separately included as seismic sources in addition to area sources, are usually attributed to their own  $b$ -values, which need to bear no immediate

relation to the values obtained from the regional recurrence statistics (Youngs and Coppersmith (1985).

### 3 Geologic and seismotectonic setting

Over the geological time scale Indian plate has moved northward and rotated in the counter clockwise direction. The collision between the Indian and Eurasian plates began some 30 to 40 m.y.b.p. (Aitchison et al., 2007) and the Tethys Ocean has entirely been consumed between the Eurasian, the Arabian and the Indian plates (Powell, 1979). Present day tectonics are marked by collision and thrusting along Main Boundary Thrust, Pamir Himalaya and the Hindu Kush region forming the northern plate boundary. On the western side the tectonics of colliding Indian and Eurasian plates are governed by transform plate boundary consisting of the Chaman and Ornach Nal fault Zone with left lateral strike-slip motion (Fig.3.1). In the southern most areas i.e. west of Ornach Nal fault zone the oceanic lithosphere is subducting below the continental crust. In terms of structural trends, the Main Boundary Thrust (MBT) and allied thrust faults form an elongated zone in NW-SE direction whereas western margin along Chaman and Ornach Nal zone exhibits a dominant North South trend. Due to compressional regime of the Arabian plate, the Chagai arc and the Makran zone have structural trends in an East West direction. The structural trends observed on local scale around Quetta have two distinctive natures. The Chaman Fault Zone on western side of Quetta city and Suleiman Arc and Sibbi Trough on eastern side of the Quetta city. To the south the Kirthar ranges, stretches south from Quetta.

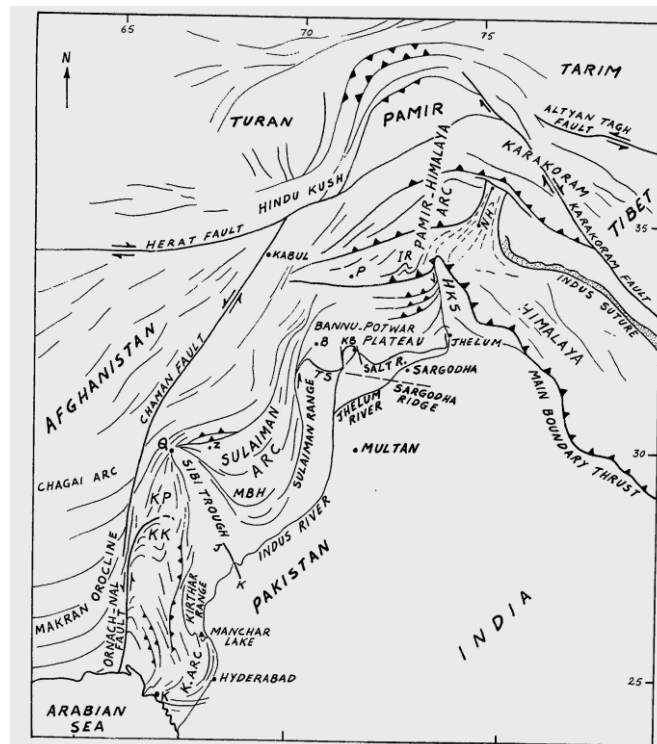


Figure 3.1. Regional tectonic map of the area. B-Bannu, HKS-Hazara Kashmir Syntaxis, J-K—Jacobabad Khairpur high, K-Karachi., KB- Kalabagh, KK- Khuzdar Knot, KP- Kalat Plateau, MBH- Mari Bugti Hills, NH-Nanga Parbat Haramosh massif, P- Peshawar, TS-Trans Indus Salt Range, Q-Quetta, Z-Ziarat (Sarwar, and DeJong, 1979).

The Chaman fault was first discovered in 1893 (Griesbach 1893) after the 1982 earthquake, which offset the Quetta-Chaman railroad by 75cm in left lateral movement. The fault is a left lateral transform fault. It is considered responsible for famous 1935 (Ms 7.7) earthquake. Lawrence and Yeast (1979) divided it into four segments. First is the *active fault* which is a linear feature and extends without interrupting the entire length of segment. Alluvial fans are cut by this segment of the fault with visible marks in areal photos over areas of bedrock. The second part is the Chaman *fault zone* is one kilometer wide, with a fault gauge and active fault zone present in this zone. The third segment is the Chaman *fault system*, which is a series of four to five branches that curve away from the main trace towards southwest and west. The fourth is the Chaman *transform boundary* which includes the Chaman, Ornach Nal and other faults that constitute the boundary between Indian and the Eurasian plates.

The Sulaiman lobe or Sulaiman arc is a broad (>300 km) and gentle (<1° sloping hills) fold-and-thrust belt that is tectonically active. It is developed by transpression as a result of the left-lateral strike-slip motion along the Chaman fault and southward thrusting along the western terminus of the Indian subcontinent (Sarwar and DeJong 1979; Lawrence et al. 1981). The present day structural style and tectonic of the Ziarat area was developed due to the interaction between Suleiman Lobe, Chaman fault and the Sibbi trough. Two major thrusts, Gogai Nappe and the Babai Nappe are also present along with associated strike slip faults (Niamatullah et al. 1989).

### 3.1 Mode of faulting around Quetta

The data about present day mode of faulting is available primarily in the form of maps and published literature. It can be validated by using earthquakes and their focal mechanism data. The Global Centroid Moment Tensor (CMT) catalogue provides focal mechanism solutions for larger earthquakes. These have been plotted on tectonic map of Quetta and surrounding regions using GMT for region between 29.00N to 31.00N and 66.0E to 68.00E. Based on the studies of tectonics and focal mechanism, following important features are determined (see also Fig.3.2 below):

- In the west of Quetta the strike slip mechanism corresponds to left lateral movement along the Chaman fault.
- Mechanism of two earthquakes (30.8N & 67.8E) in the north of Quetta are pure thrust faults, which corresponds to the Chiltan fault system, and is characterized as a thrust fault on the tectonic map.
- An additional feature not reported previously on tectonic maps and literature is named as the “Mach Structure”. Following Rafi et al (2011), it is included in the fault model for the hazard computation. Rafi et al. (2011) reported seismic activity, primarily based on historical evidence, along a northwest southeast trending structure with dominant strike slip movement. The same structure was considered as responsible for the Quetta-Ziarat Earthquake of 29th October 2008. The findings by Rafi et al (2011) are further supported by alignment of historical seismicity along the Mach Structure as shown in Fig. 6.10.

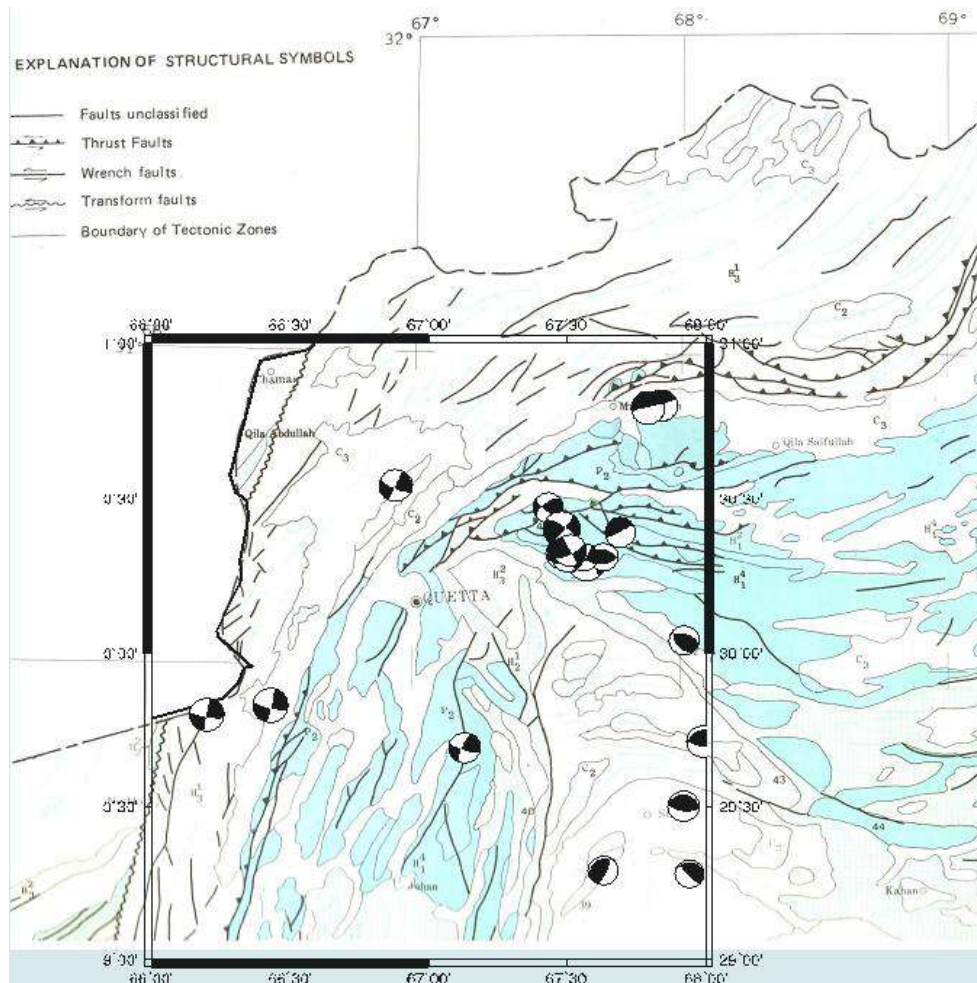


Figure 3.2. Focal mechanism solutions obtained from the CMT database for the region of Quetta (<http://www.globalcmt.org/CMTsearch.html>).

#### 4 Earlier seismic hazard and zoning results

The following three important studies for seismic hazard analysis are available:

1. According to Aron Josha (2009) it is estimated that Quetta city at 2% probability in 50 years is expect a PGA of 0.67g (corresponding to  $6.6 \text{ m/s}^2$ ), with highest values estimated for Sheikh Manda and Chiltan Housing Society.
2. As per the building codes of the Pakistan Seismic Provision 2007 (BCP SP 2007) the Quetta district and its Tehsil Panjpai (S/T) are located in zone 3 with the highest design values of 0.32g for this zone. Areas in south which include Mastung and Mach are also in Zone 3. Whereas, the areas north of Quetta, including Pashin Muslim Bagh and Ziarat in North East are in zone 4. Building codes of Pakistan (BCP SP 2007) recognized as official building code for the country and for Quetta also.
3. Probabilistic seismic hazard study was conducted by Pakistan Meteorological Department and NORSAR in 2007 for the entire country. Expected PGA for Quetta for return period of 500 years is given as  $3.85 \text{ m/s}^2$ . Analysis by PMD was based on  $1^\circ \times 1^\circ$  grid and is very coarse to estimate hazards at local level.

## 5 Assessment of earthquake potentials

### 5.1 The largest earthquakes within the greater area

#### *1931 Sharigh Earthquake*

The earthquake on 24<sup>th</sup> August 1931 with a surface wave magnitude  $M_s$ 6.8 and depth of 33Km. It was followed by the  $M_s$ 7.3 Mach earthquake. It has been difficult to obtain the intensity reports because at most places the second shock was far more destructive of the two. The information for intensity distribution of Sharigh earthquake was reported to be incomplete by West (1934). The earthquake had intensity VI at Quetta and Harnai with maximum documented intensity of VII at Mushkaf.

#### *1931 Mach Earthquake*

The Mach Earthquake occurred on 27<sup>th</sup> August 1931 with a magnitude of  $M_s$ =7.3 (Ambraseys and Bilham, 2003) with a reported depth of 33 Km and was felt in Baluchistan and Sindh (550 km distance). Approximately 120 deaths occurred due to this earthquake. West (1934, 1937) has reported the maximum intensity of VIII. Most of the damage was reported in Mach. All the buildings in New Mach were damaged to some extent while many houses, built from the dried mud bricks (adobe) or stone with mud mortar, were completely destroyed along with two government rest houses. The bazaar, some of the railway residences at new Mach, and the outlying village of Old Mach was also heavily damaged. At the time of earthquake, the train stationed at Mach swayed from side to side the driver was thrown from the engine, but the trains did not overturn. In old Mach destruction was more extensive and most of public buildings were totally destroyed. Five people died, and the total damage to the inhabitants was not more the Rs.70000. There were reports of large rock falls, from mountains in the north of Mach, rising big clouds of dust leading to rumors of volcanic eruption. The rail bridge 140 m long in Mach remained safe. West (1934, 1937) reported that the track southeast of the bridge, which was on level settled due to gradual lowering of southeast segment of track by 60 cm. The bridge was compressed and shortened by 20 cm.

In a more recent research Szeliga et al. (2009) have concluded that the earthquake occurred on a 42 km wide east-west and 72 km long North-south Dezghat/Bannh fault system situated in the west of Sibbi. The fault slipped in a reverse sense to the east with maximum slip of 3.2 m and a mean slip of 1.2 m. They have also promoted (argued for) a mechanism that stored elastic strain from past events which account for a 3.2 m of local slip observed up dip from the inferred locking line of the 1931 earthquake.

#### *1935 Quetta Earthquake*

The famous Quetta Earthquake of 1935 originated on 30<sup>th</sup> May with an estimated surface wave magnitude of 7.7 (Ambraseys and Bilham 2003) four years after the Mach earthquake due to unclamping of fault by the earlier earthquake (Mach 1931). A total of 35000 people died in this earthquake. Out of these, 26000 people were killed in total in Quetta. In Kalat tribal areas some 8410 people died. This was the deadliest earthquake in the subcontinent of Pakistan before the occurrence of 8<sup>th</sup> Oct 2005, Kashmir earthquake. Quetta city was the most damaged area. Quetta was divided into two major parts at that time, the cantonment (military compound) and the civil areas. 15000 people died in the civil area of Quetta city (Pinhey 1938). All important buildings were destroyed except some reinforced concrete structures and the railway quarters, constructed after implementation of the 1931 earthquake resistance

design. The cantonment areas remained comparatively safe while church and military hospitals remained intact. In the state of Kalat, 2900 people out of its population of 10000 died and 5000 were injured. All villages between Quetta and Kalat were destroyed with 70% of population either dead or injured.

The earthquake was most likely associated with a zone of faults that lie along east edge of the Chiltan Range and it passes to south near Mastung and Kalat. Ambraseys and Bilham (2003) has placed the epicenter at 160 km south of Quetta, about 40 km west of Kalat, with an estimated seismic moment of  $17.0 \times 10^{27}$  dyne cm.

## 5.2 Earthquake catalogues

Earthquake catalogues are the main information source for the present hazard evaluation. The catalogues used in this study are established from reports of various international agencies that have been and are in operation over a fairly long time. This is important because the length of the catalogue is essential, with fairly long recurrence times of the largest earthquakes.

Three main catalogues have been used as basis for the present study:

- ISC catalogue (*International Seismological Centre, 2009*):.
- PDE (NEIC) catalogue (*USGS, 2009*):
- CMT catalogue (*Harvard Centroid Moment Tensor Project, 2009*):
- PMD catalogue

### 5.2.1 Historical earthquakes

The Quetta region shows a remarkable pattern of the historical earthquakes as shown in Fig. 5.1. These earthquakes clearly demarcate a NW-SE trend that runs nearly parallel with the instrumentally recorded earthquakes (captured with the zone), but still with a clear separation. We do believe that this distinction between instrumental catalogues and the historical seismicity is real; i.e. that the relative location of the large historical earthquakes is not biased by erroneous locations (although we cannot exclude that possibility). The historical earthquakes that form this line are tabulated in Table 5.1.

It should be observed that none of these earthquakes occurred prior to 1867 and it is noteworthy to observe that the instrumental seismicity (Fig. 5.2) clearly depicts the neighbouring region to the north as more active.

The historical data indicates that we had seven very large earthquakes in about thirty five years (1867-1904). This high seismic activity may indicate activity along a hidden lineament. Our interpretation of the concentration along a line and the relative time-cluster is that there exists a deeper lineament (as indicated on geological maps), the large historical earthquakes occurred through some sort of connections along this line. This interpretation is later used for modelling a fault line (see below).

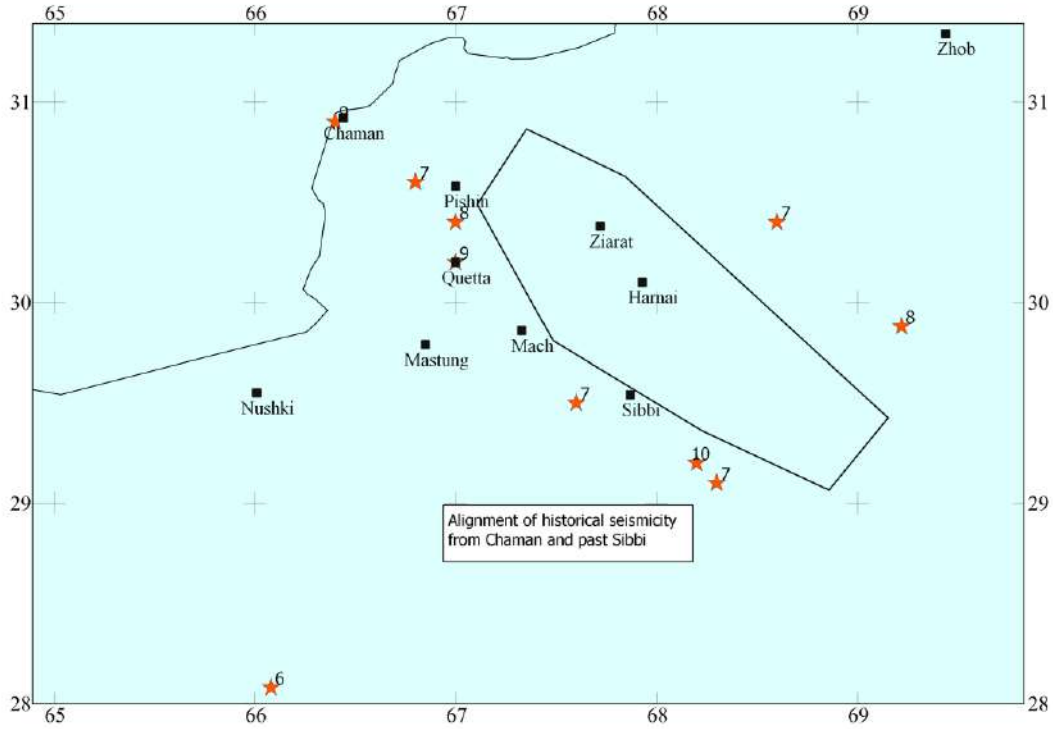


Figure 5.1. The location of historical earthquakes that mark a line from Chaman and past Sibbi. The zone indicates where today’s instrumentally recorded seismicity is concentrated. See Table 5.1 for the details of these historical earthquakes.

**Table 5.1.** Historical earthquakes that form the NW-SE line crossing the Quetta region from Chaman across Sibbi as also depicted in Fig. 5.1. Maximum Intensity is indicated with normal numbers (not Roman as is customary).

Day	Month	Year	Lat	Lon	Max I (roman)
-	-	1867	29.1	68.3	VII
15	12	1872	29.2	68.2	X
20	12	1892	30.9	66.4	IX
13	2	1893	30.2	67	IX
-	-	1900	30.4	67	VIII
-	-	1902	30.6	66.8	VII
23	12	1903	29.5	67.6	VII

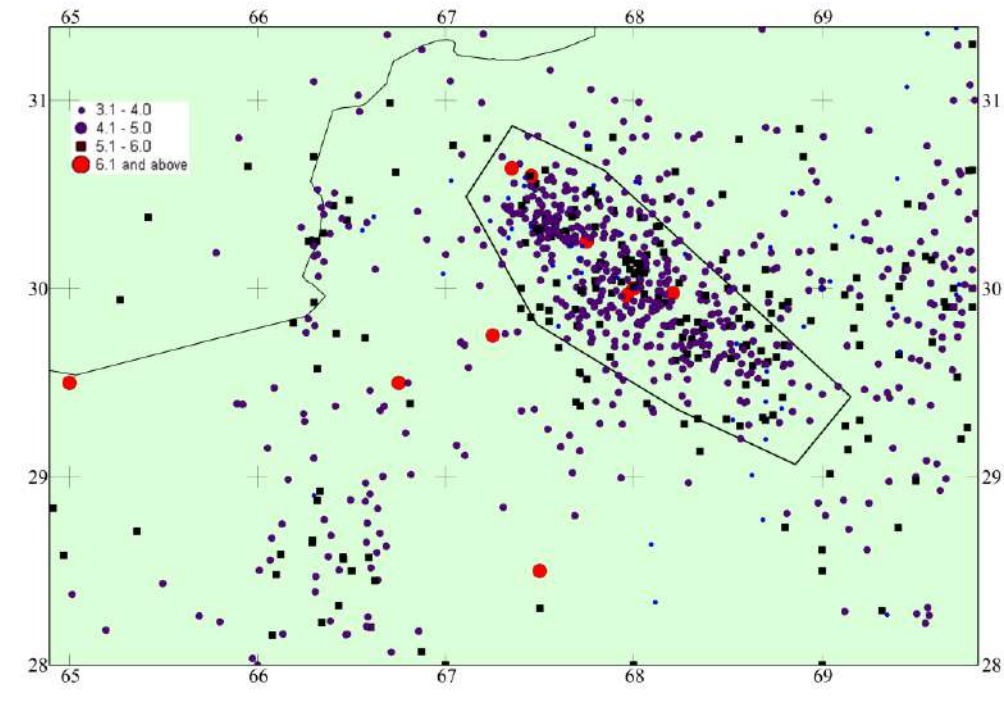


Figure 5.2. The location of instrumental earthquakes (ISC data).

### 5.3 Geographical distribution of earthquake databases

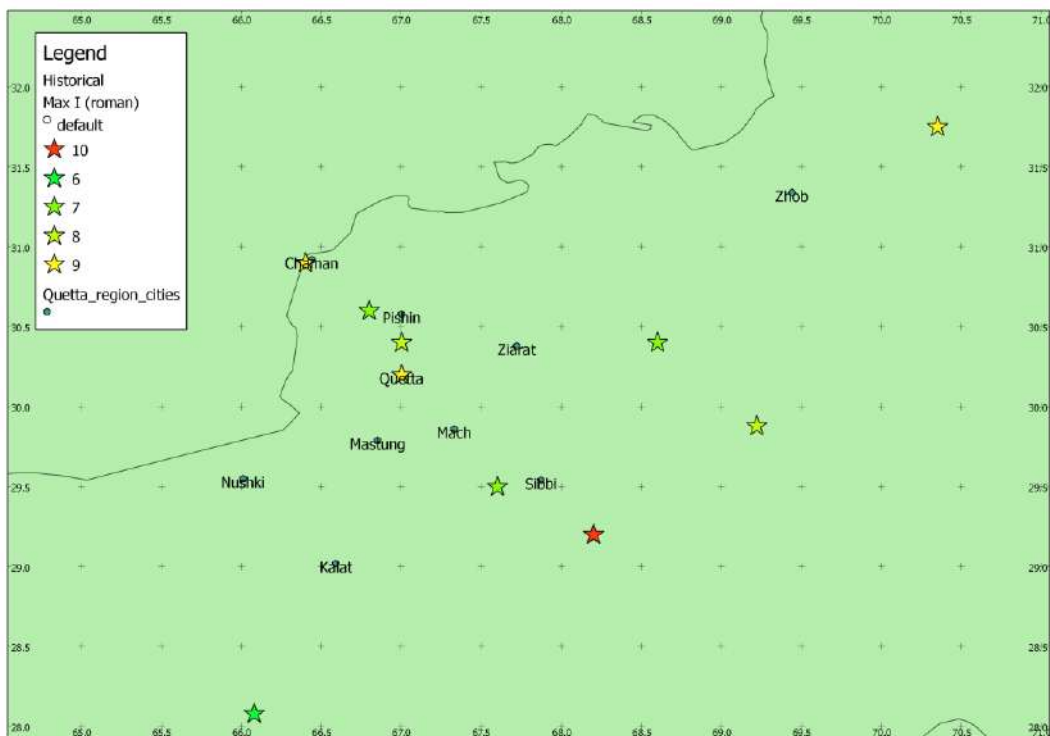


Figure 5.3. The location of historical earthquakes before 1904 in the PMD database. The alienation of earthquakes between Chaman and Sibbi cities are remarkable.

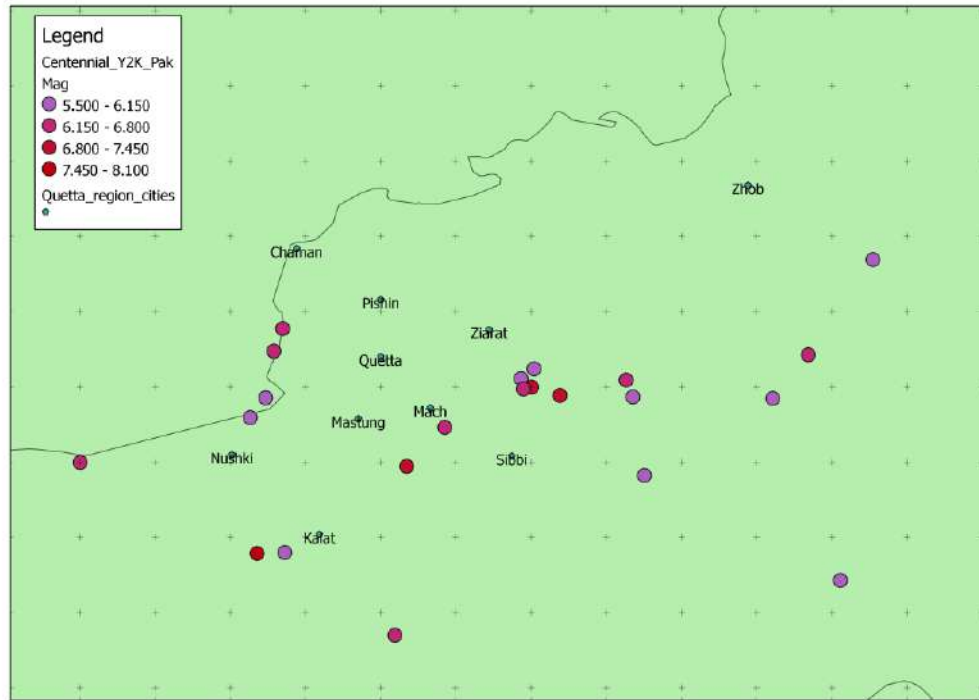


Figure 5.4. Distribution of the largest earthquakes in the Centennial (EHB) catalogue (1900-2000).

## 6 Seismotectonic zonation and quantification

### 6.1 Magnitude conversions

A homogenized magnitude is prerequisite for statistical analysis of the earthquake catalogues. Since the catalogues at hand are often using and reporting a mix of magnitudes we undertook the conversion of all magnitudes into a homogenized moment magnitude using relations developed by Scordilis (2006).

Data have been collected from ISC, USGSPDE and PMD catalogues for analysis. Earthquake data reported contains both body wave and surface wave magnitude along with moment magnitude for some large events. Original moment magnitudes  $M_w$  have been kept as reported by the agencies. In order to homogenize the different types of magnitudes the other magnitudes have been converted to moment magnitude by using the relations defined by Scordilis (2006), and is given below;

For  $M_s$

$$M_w = 0.67 M_s + 2.07$$

$$\text{for } 3.0 \leq M_s \leq 6.1$$

$$M_w = 0.99 M_s + 0.08$$

$$\text{for } 6.2 \leq M_s \leq 8.2$$

For  $m_b$

$$M_w = 0.85 m_b + 1.03$$

$$\text{for } 3.5 \leq m_b \leq 6.2$$

There is a complete linear relation (Fig 6.1) for conversion of magnitude from  $m_b$  and  $M_s$  to  $M_w$  in the ISC catalogue. Note that the Scordilis relations for  $m_b$  to  $M_w$  conversion is valid only up to  $m_b=6.2$ . As seen from Fig. 6.1 we have slightly violated the relation by including a few larger earthquakes (for which we did not have any well founded relation).

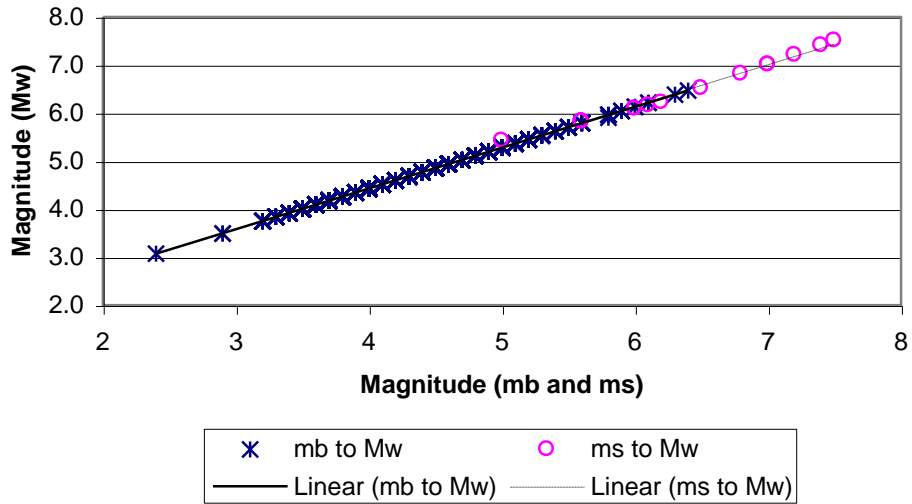


Figure 6.1. Conversion of magnitude mb and Ms to Mw from the ISC catalogue.

The catalogues were converted using the following scheme of preference:

- 1) First priority: Whenever a Mw was originally reported this was used (preferably ISC derived Mw in the ISC catalogue).
- 2) Second priority: The mb was converted to Mw whenever available.
- 3) Third priority: The Ms was converted to Mw whenever available.

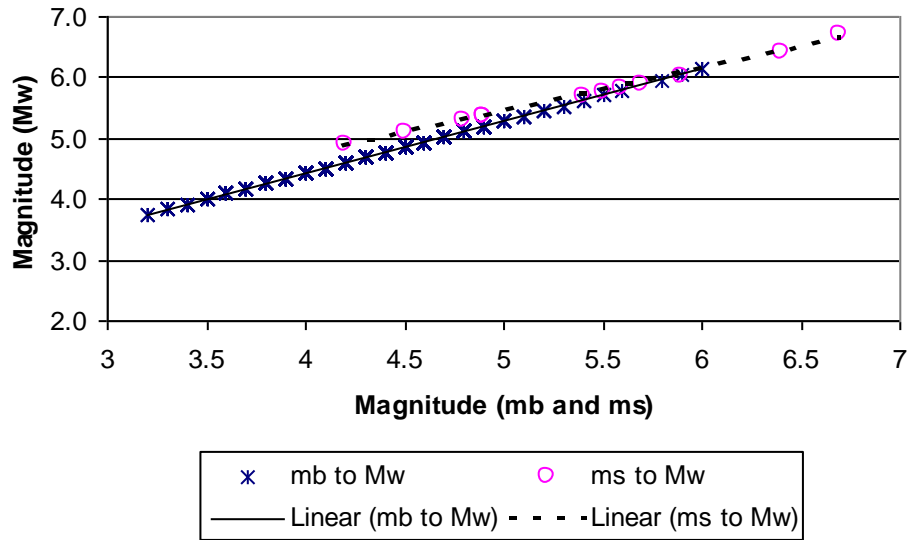


Figure 6.2. Conversion of magnitude mb and Ms to Mw from USGS-PDE catalogue.

### 6.1.1 Some manual magnitude assessments

The largest earthquake of Quetta, 1935 and some others have been analyzed in by various authors. We adopted the principle to override the catalogue reported earthquakes for the following ones (where we adopted magnitudes from Ambraseys and Bilham (2003):

**Table 6.1.** Detail of earthquakes with manual magnitude assessment from Ambraseys and Bilham (2003).

Month	Day	Year	Lat	Long	Depth	Mw used
5	30	1935	29.5	66.75	35	7.7
8	27	1931	29.75	67.25	35	7.3
8	24	1931	30.25	67.75	35	6.8

## 6.2 Completeness, aftershocks and magnitude-frequency relation

### 6.2.1 Aftershocks

Aftershocks from large earthquakes are certainly herein the analyzed catalogues. However, frequent aftershocks are experienced due to the fact that one large earthquake may trigger larger earthquakes on neighbouring, and even in the quite distant faults, that are expected within weeks and months after the occurrence of first large earthquake. These are not aftershocks, but rather “offspring” earthquakes triggered by the region stress-change. This observation has been observed since long and is also nicely documented in Ambraseys and Bilham (2003).

As for real aftershocks we have not made efforts to remove these from the catalogues before processing. The reasons for this is that in the Quetta region none of the catalogues (USGS and ISC primarily) have with the location precision that allows distinction between an earthquake occurring as an aftershock on the main rupture, or belonging to neighbouring faults, triggered by the general stress-restructuring of a larger crust volume. If we had undertaken the challenge to remove aftershocks, the likelihood of also removing genuinely triggered earthquakes on neighbouring faults would have been significant. As a result of our approach it is likely that the analyzed catalogues have included some genuine aftershocks, and this may explain (see below) why the b-values are somewhat higher than the globally expected value of 1.0. This is a choice we have made; it has some advantages (not removing genuine earthquakes), and some disadvantages (leaving some aftershocks in the catalogue).

### 6.2.2 Completeness

Before conducting statistical analysis on any earthquake catalogues its completeness within the time and magnitude bounds within which the analysis is to be conducted must be confirmed. There exists several mathematical techniques for such analysis (beginning with the famous Stepp analysis (Stepp et al. 1973). Nearly all of the mathematical based analysis are based on the assumption of a log-linear magnitude-frequency distribution such that completeness windows are defined from a log-linear compliance criteria. In the present investigation we have refrained from using such analysis tools as we find the eye, very sensitive to changes when earthquakes are plotted in magnitude-time plot. Consequently this technique has been used as preferred in this investigation.

In order to check the completeness of the earthquake data catalogue a simple technique was adopted in which data was divided into different periods and plotted against magnitude Mw. A simple formula given below was utilized to have uniform values for time from date, month and year of occurrence of the earthquake.

$$\text{Time} = \text{Year} + ((\text{Month}-1) * 30 + \text{Day}) / 360$$

Based on the data exemplified in Figs. 6.3-6.6 we could determine the completeness of the USGS and the ISC catalogs.

The ISC catalogue is considered to be complete for magnitude 6.2 and above for period 1909 onwards. The data in lower magnitude range is available from 1961 with first reported earthquake of magnitude below 5.0 however bulk of input of data starts from 1964 and catalogue is considered to be complete for magnitude 4.5 and above for the duration 1965 onwards. There is a pattern of reduced seismic activity from 1967 to 1978 for which reason can be old instrumentation. For magnitude 4.0 and above ISC catalogue is considered to be complete from 1995.

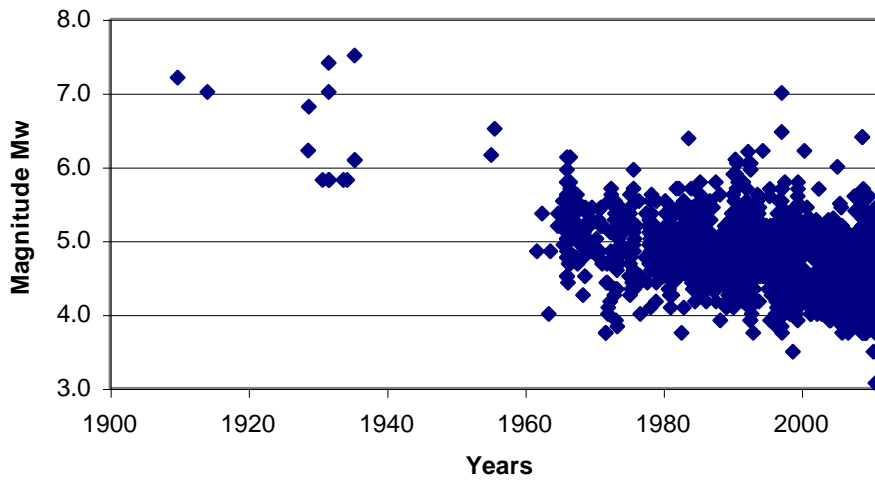


Figure 6.3. Time distribution of magnitudes in the ISC catalogue for the period 1900-2000.

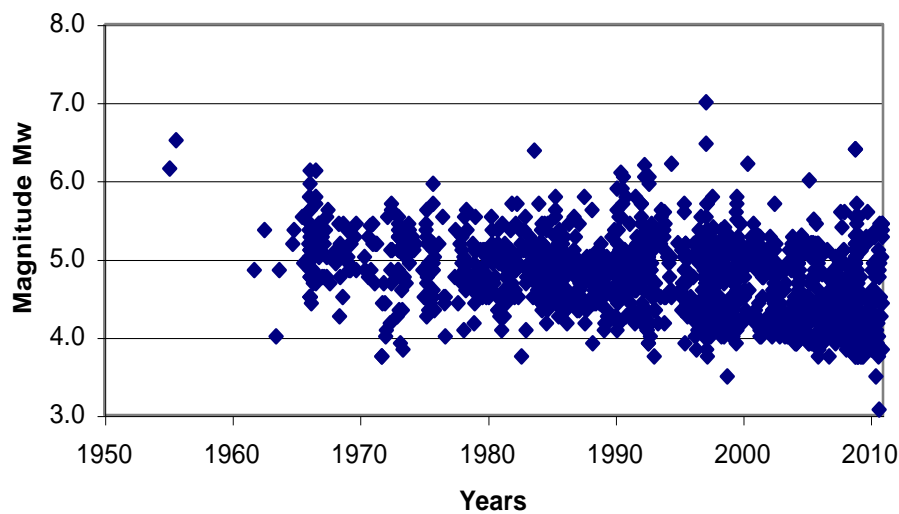


Figure 6.4. Time distribution of magnitudes in the ISC catalogue for the period 1950-2010.

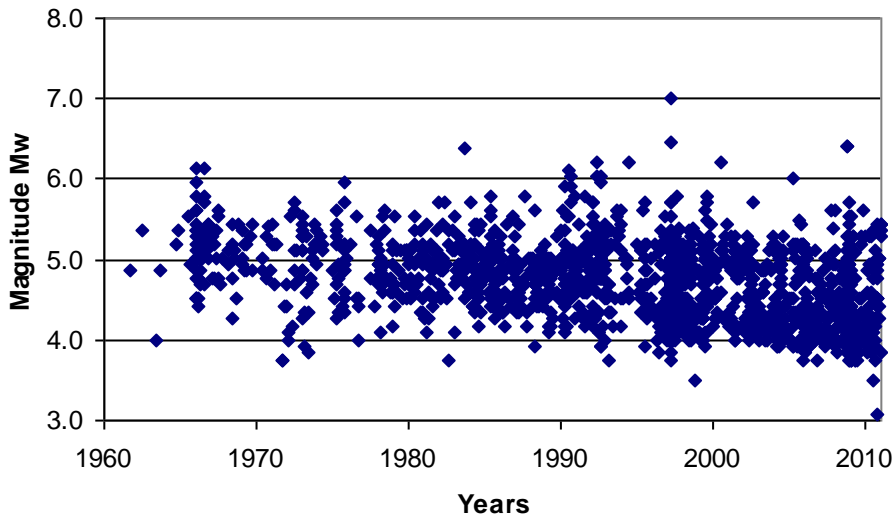


Figure 6.5. Time distribution of magnitudes in the ISC catalogue for the period 1960-2010.

USGS PDE provided data from 1973 onwards for the area. For initial period up to 1978 earthquake frequency is lower compared to rest of the duration. However the catalogue can be considered complete for magnitude 5.0 and above from 1973 whereas it is complete for magnitude 4.2 and above from 1992 onwards.

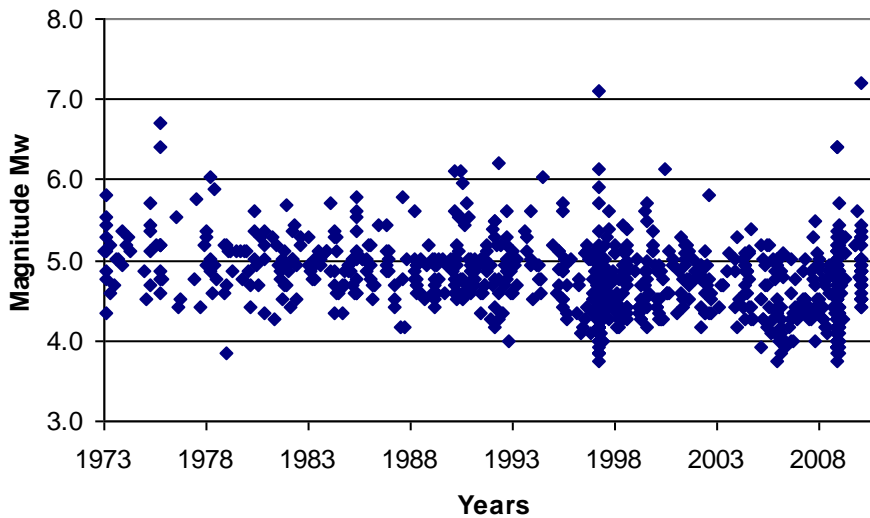


Figure 6.6. Time distribution of magnitudes in the USGS catalogue for period 1973-2010

### 6.3 Seismic zonation

The zonation was primarily based on two instrumental catalogues, the ISC and the USGS catalogues. The following features can be recognized (e.g. Fig. 6.10):

- From south the seismicity follows a N-S trend along the Kirthar ranges.
- At Chaman (north of Quetta) the seismicity continues northward along the Chaman fault zone in a somewhat disperse way. A smaller region NW of Quetta (probably on the Chaman fault exhibits quite extensive seismic activity.
- The seismicity is most intense along the southern bend of the Suleiman range where it covers an elliptical area that stretches NW – SE north of Quetta, Mach and Sibbi.
- As the Suleiman range bends in a NE direction and continues northwards the earthquake activity is less intense and less spatial concentration (covering a larger area).

By and large, the points as describe above shows that how the seismicity clearly follow the mountain ranges and reflect the large scale tectonic patterns.

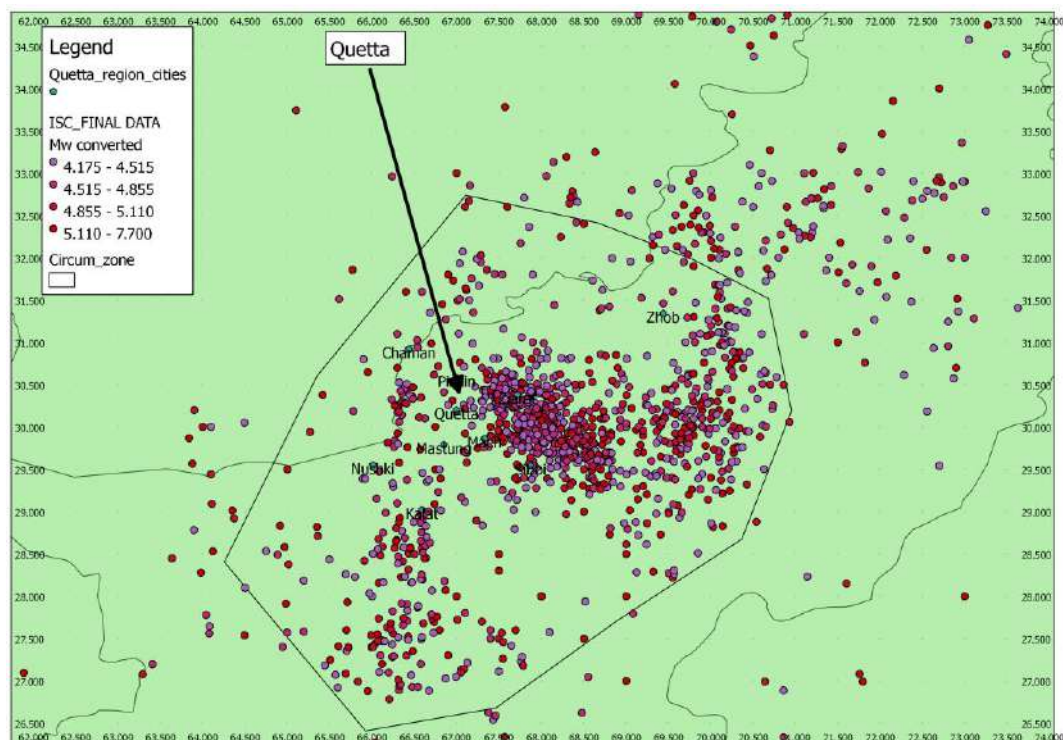


Figure 6.7. Earthquake distribution around Quetta as seen from the ISC catalogue.

Based on the above points a quite simple zonation as shown in Fig. 6.8 was used as basis:

- The Main zone: Defining the zone of most intense activity
- The North zone: Defining the zone of high activity largely related to the Suleiman range.
- The South zone: Defining the zone south of Quetta and largely defining the activity related to the Kirthar range.
- The West zone: Defining the recent intense activity that seems to take place on the southern end of the Chaman fault.

- The remaining eastern and western zones (large) comprise the more diffuse earthquake activity outside the defined zones.

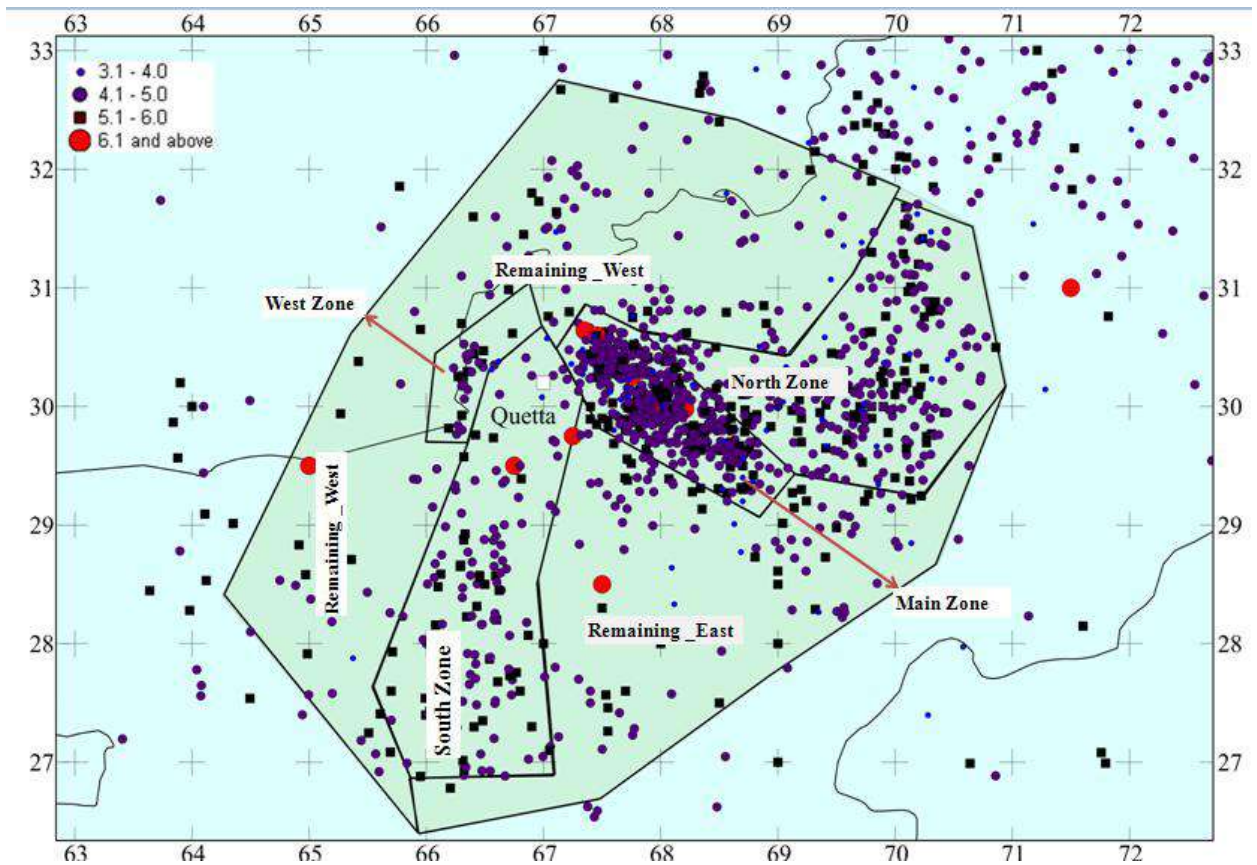


Figure 6.8. Zones defined as basis for the present hazard investigation.

### 6.3.1 The local faults included in the hazard model

There are different sources available for acquiring details of the local fault systems in and around the Quetta region, and one example are the tectonic and fault maps by Ali Hamza Kazmi (1979) and the Geological Survey of Pakistan (GSP). However these maps from Hamza and GSP were preliminary and not updated after their publication. In a recent work at the National Center for Geology in the Peshawar University, research is under way to mark all the faults of Pakistan and to prepare an updated map. For the present study the Peshawar University has provided the fault map as given in Fig. 6.9 by Khan et al. (2012). The details of the some selected faults are given below:

- **Chaman Fault:** The Chaman fault (or fault group) stretches sub N-S until it meets the Herat fault in the north. The Chaman fault has a left-lateral strike slip feature and has not released energy in a regular high earthquake activity in recent past. Ambraseys and Bilham (2003) speculate there is a significant accumulation of stress that has made this structure ready for one or more major earthquakes.
- **Kalat – Chinjin Structure:** The Kalat fault starts north of Anjira town, continues in the northward direction passing through Kalat town and west of Quetta city. It further continues by change in orientation in a northeast direction. The reported length of the Kalat fault is 107 km with a dip in a west-northwest direction. The structure continues under the tectonics of the Suleiman arc in the east direction where it is called as Chinjin-Zakriazi thrust. This portion has a strike of 234

degrees and is also in northwest direction. These are considered as two different faults but in the present study the Kalat fault and Chinjin-Zakriazi thrust have been merged and modeled as a single structure named as Kalat-Chinjin structure.

- **Harnai – Tatra Structure:** The fault “starts” in the area between Kach and Khost towns. It has a length of 140 km with a northwest-southeast orientation and passes close to Harnai. It further continues in SE direction till it bends and aligns in almost east-west direction. The dip of the fault is estimated in a northeast direction.
- **Ghazaband – Zhob Structure:** The Ghazaband – Zhob structure is also modeled as a single fault similar to the Kalat-Chinjin structure. It lies parallel to the Chaman fault and the Kalat - Chinjin structure in the south but bends in the north by coupling the Kalat - Chinjin structure to the Suleiman lobe. The dip direction is southeast (opposite to the Kalat-Chinjin fault).
- **Mach Structure:** This structure is not previously described in literature and geological / fault maps. It has been included in the study keeping in view of the results of Rafi et al (2011). This study indicated a northwest southeast structure and is contrary to previous descriptions of the area as thrust. This structure is poorly recognized by surface manifestations; however, the large historical earthquakes seem to align along this structure. It may be responsible for the recent Quetta-Ziarat earthquake of magnitude 6.5mb with a foreshock of magnitude 5.0mb. The structure runs tentatively from the Harnai – Tatra fault in a southeasterly direction and pass close to Sibbi.

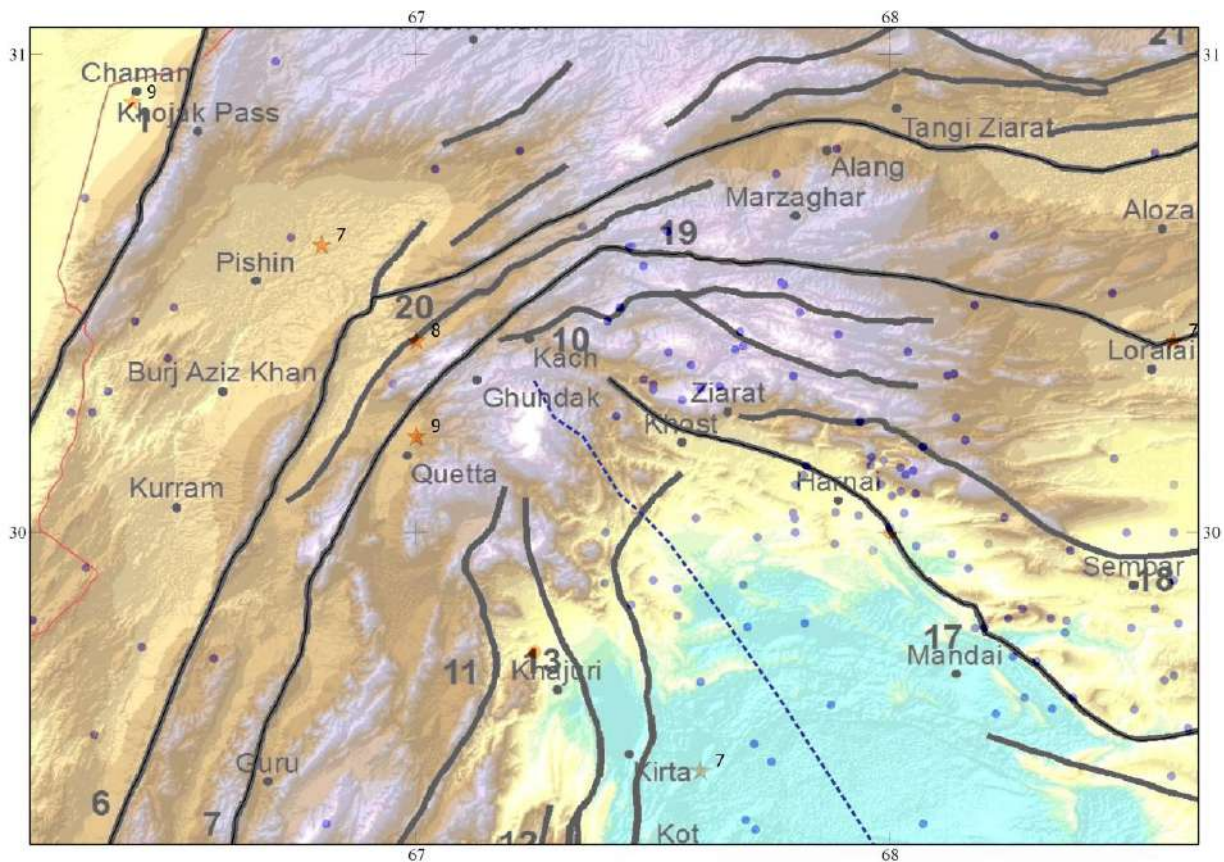


Figure 6.9. Structural map of the region surrounding Quetta, Balochistan. Base Map modified after Khan et al (2012). (Red Stars: Historical Earthquakes with intensities, blue circles: seismicity above magnitude 5.0 from ISC, Thick Black Lines: faults, dashed blue line: Mach Structures

In addition several smaller faults can be identified as splays or associated faults in the complex fault pattern that forms an arch around Quetta. The faults used as basis for the PSHA modelling are shown in Fig. 6.10.

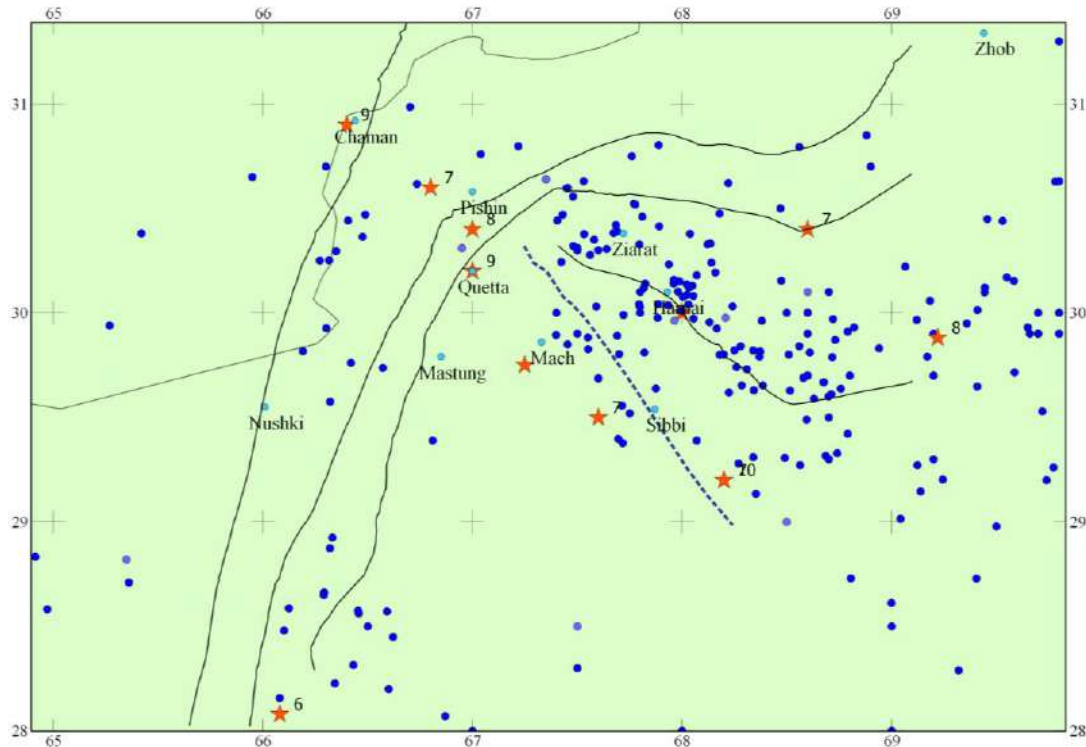


Figure 6.10. Local and regional faults in the vicinity of Quetta used in the present study, both as background and as direct quantifiable in terms of hazard. Note 1: The Chaman fault line that stretches northwards until it meets the Herat fault in Afghanistan is the major strike-slip fault with a major potential. Note 2: The Mach line stretching SE from Quetta is not really a fault, but rather a geological lineament. It is included here because of its apparent importance in the historical earthquake database. Note 3: The other local faults are included as an approximation of the dense fault pattern observed by field geologists in this area.

#### 6.4 Model parameters

The regressions for recurrence parameters (Gutenberg-Richter) were conducted independently on two catalogues (ISC and USGS; PDE). The Gutenberg-Richter regression was further conducted on a larger zone comprising the area around Quetta (Fig. 6.11 & 6.12). For these catalogues completeness analysis results were used for constraining time and magnitude cutoffs as follows:

1. For the ISC catalog (instrumental starting from 1909) the following periods of completeness were determined:
  - a. From 1909 and onwards for  $M \geq 6.2$
  - b. From 1965 and onwards for  $M \geq 4.5$

- c. From 1995 and onwards for  $M \geq 4.0$
  - d. Certain “gaps” were noted in the distribution of earthquake magnitudes as function of time of occurrence (see above), but these gaps could well be related to some natural seismic paucity and were therefore interpreted as natural.
2. For the USGS catalog (instrumental starting from 1974) the following periods of completeness were determined:
    - a. From 1974 and onward for  $M \geq 5.0$
    - b. From 1992 and onward for  $M \geq 4.2$

For these 5 time and magnitude windows of the catalogs regressions were conducted in order to obtain the Gutenberg-Richter recurrence relation:  $\log(N) = a - b \cdot M$  (in our case  $M_w$ ). The results for the ISC catalog are shown in Fig. 6.11 and for the USGS catalog in Fig. 6.12.

The results from the two catalogs yielded the following independent relations for the larger area around Quetta:

- $\log(N) = 6.506 - 1.1422 \cdot M_w$  (ISC data)
- $\log(N) = 6.500 - 1.1327 \cdot M_w$  (USGS data)

These results are regarded as remarkably uniform given that the catalogues are obtained on independent data and the magnitudes were homogenized from different magnitudes types. Based on these results we concluded that for the circum region around Quetta the Gutenberg-Richter relation was reliably established to:

$$\log(N) = 6.5 - 1.14 \cdot M_w$$

The uncertainties in these results are nevertheless recognized since we are dealing with very short time windows. Uncertainties are therefore introduced in the PSHA scheme.

#### ***A comment on the b-value***

It is noted that the b-value of 1.14 is well established through the instrumental catalogs, however at the same time it is recognized to be in the higher end of expectations. Compared with some earlier investigations (e.g. Ambraseys and Bilham, 2003) it is clearly high. We do accept this, but at the same time attribute this to the possible inclusion of aftershocks as explained above were not removed due to the risk of removing too many other earthquakes.

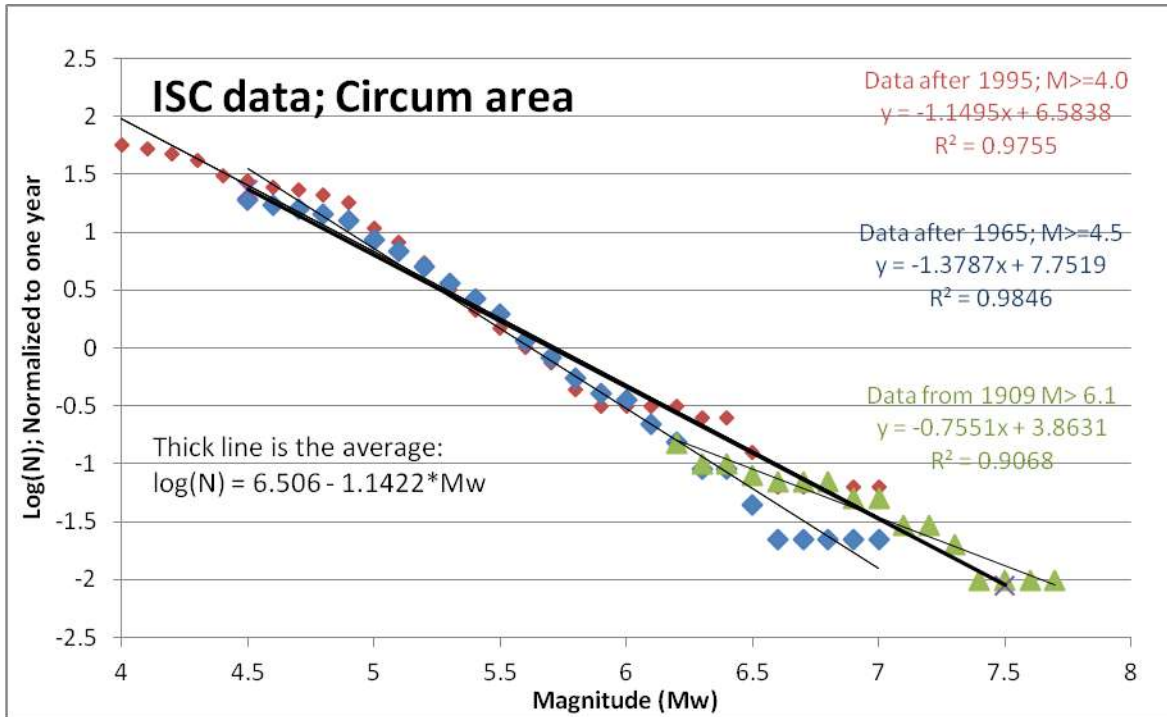


Figure 6.11. Gutenberg-Richter regressions conducted on 3 independent time and magnitude windows of the ISC catalog. Thick line represents the average. All data were normalized to 1 year.

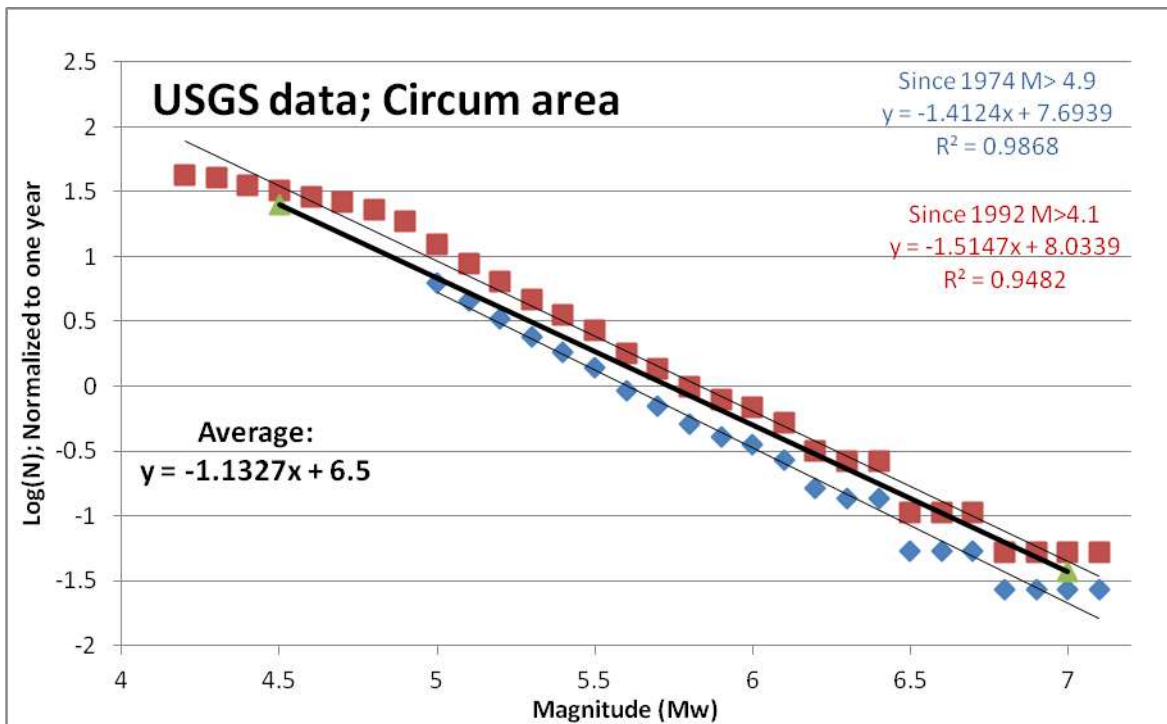


Figure 6.12. Gutenberg-Richter regressions conducted on 2 independent time and magnitude windows of the USGS catalog. Thick line represents the average. All data were normalized to 1 year.

### 6.4.1 Zonation and distribution of activity

The calculation of recurrence relations for individual zones is often conducted by individual regressions on data within each zone. While this is recommended it may also lead to inconsistencies as b-values may come out differently and thereby shift the overall moment release budget. Since it is quite important to respect the overall moment release budget we have taken another approach. Within each zone we have counted (for the various catalogues) the number of events equal or greater than 5, 6 and 6.5. While some differences occur these simple numbers provide a good image of the relative energy release within each zone.

The results for the circum zone and for the four defined subzones were as follows:

**Table 6.2:** Definition of areas (absolute and relative) within the zones defined.

	Area (sqkm)	Area (%)	Average activity %
Circum zone	292672		
Main zone	16408	5.60627597	39%
South zone	42624	14.5637437	15%
West zone	6168	2.10747868	13%
North zone	40616	13.8776514	09%
Remaining (east & west)	186856	63.8448502	25%

Remaining indicates the difference between the defined zones and the total circum zone.

Using the above obtained values it was possible to define activity for the four zones as follows:

**Table 6.3:** Recurrence values used in the computational model as established through regressions on the data; N-value corresponds to an  $M \geq 5.0$  earthquake. The return period (in years) is given for each zone is for  $M=6.0$ .

	b	N	a	T=6	T=5
Main zone	1.14	2.43166156	6.08590313	5.67	0.41
South zone	1.14	0.92001915	5.66379687	15.00	1.09
West zone	1.14	0.84183517	5.62522707	16.40	1.19
North zone	1.14	0.56981026	5.45573027	24.23	1.75
Remain_east	1.14	0.61216549	5.48686884	22.55	1.63
Remain_west	1.14	0.93408181	5.67038492	14.78	1.07

### 6.5 Fault modeling

It is very clear that the empirical data for PSHA investigation is extremely short compared to the probabilities of interest in a standard hazard investigation which are normally around 500 years recurrence, corresponding to  $0.002 \times 10^{-3}$  annual exceedance rates. For this reason it was decided to also include some local faults as contributing to the hazard of Quetta. While there exists evidence that indeed these faults and structural zones are seismically active, the actual recurrence or quantification of the earthquake activity of these faults remains uncertain (at the best). The way these faults are included in the PSHA model is therefore reflecting more on expert opinion than on facts. The following faults are included in the hazard modeling (see also Fig. 6.13):

**Table 6.4:** Parameters of fault modeling for the hazard analysis of Quetta. The total seismic moment release from the faults is less than 10%.

Fault name	Modeled activity at M=7.3	b-value	Minimum and Maximum magnitude expected	Mode of faulting
Chaman fault	$\Lambda = 0.00057$	0.80	7.3 – 7.8	Strike-Slip
Kalat-Chinjjin fault	$\Lambda = 0.00057$	0.80	7.3 – 7.8	Reverse
Harnai – Tatra Fault	$\Lambda = 0.00057$	0.80	7.3 – 7.8	Reverse
Ghazaband – Zhob fault	$\Lambda = 0.00057$	0.80	7.3 – 7.8	Reverse
Mach structure	$\Lambda = 0.00057$	0.80	7.3 – 7.8	Strike-Slip

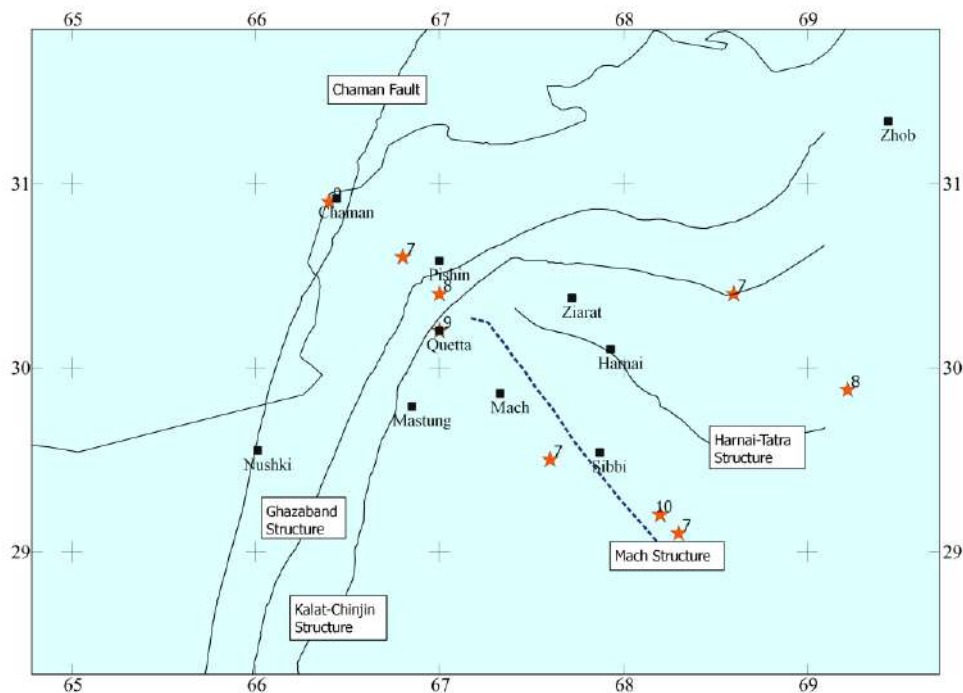


Figure 6.13. Local faults modeled in the present PSHA analysis.

A particular note on the mode of faulting: a) The Mach structure is modeled with strike slip faulting. This is choice that may forego the possible thrust movements in this region, and is based on the historical earthquakes and finding of Rafi et al (2011). b) The Kalat fault is modeled as a reverse faulting structure.

In terms of rupture length as function of fault type, the Wells and Coppersmith (1994) relations were applied.

## 7 Ground-motion models

It is well known from many earlier studies that the uncertainties in the wave attenuation models contribute significantly to the absolute hazard level and to the total uncertainty in the seismic hazard estimates, (e.g. Akkar and Bommer, 2006). The most important factor in this sense is the aleatory uncertainty, since in the hazard computations we integrate directly over the distribution described by the scatter i.e. sigma value in the ground motion model. The scatter is therefore nearly as important as the mean with respect to contribution to the total hazard.

## 7.1 General review of models

One complicating factor in the present study is that we need spectral attenuation relations, i.e., spectral relations for a suit of frequencies. Such relations are much fewer than PGA relations, and no such relations are based on Pakistan data for the Pakistan region.

There are spectral relations available for:

- Transcurrent or strike-slip regimes (e.g., Boore *et al.*, 1997), in particular California where strong motion data, including in the near field, are in abundance as compared to any other region in the world. Such regions include also important compressional conditions (revealed for example in hidden thrusts), as seen in many of the recent larger earthquakes (such as 1989 Loma Prieta and 1994 Northridge).
- Intraplate regions (e.g., NORSAR and Risk Engineering, 1991; Atkinson and Boore, 1995; Toro *et al.*, 1997), where the conditions are quite different because of insufficient empirical data, moreover it has to be based more on simulations and theoretical models.
- Compressional tectonics, where little as mentioned is available for the Himalayan region and where the closest we get is the Mediterranean region (Caillot and Bard, 1993; Ambraseys *et al.*, 1996; Ambraseys *et al.*, 2005; Akkar and Bommer, 2007). Tectonic conditions there are admittedly different, but still reasonably close to be good candidates.

The relations discussed above have been studied in detail at NORSAR, and found that sometimes there is as much difference between relations assumed to cover the same region, as there are differences between tectonically different regions. There is usually no such thing as a 'best relation'.

## 7.2 Considered models

The following ground motion models have been considered initially:

- Ambraseys *et al.* (2005) provides spectral ground motion prediction based on 595 horizontal records from shallow earthquakes in Europe and the Middle East for magnitude  $M_w$  greater or equal to 5.0 and distance range 0 to 100 km.
- Akkar and Bommer (2006) provides spectral ground motion prediction based on 532 strong motion records, that largely overlap with the Ambraseys *et al.* (2005) dataset. The disadvantage is that this relation deals with spectral ground velocity rather than with acceleration.

We finally ended up with a preference for the Ambraseys *et al.* (2005) relation. This relation is based on a large and qualitatively secure dataset. Figs. 7.1 and 7.2 shows in this

respect a comparison between the two models for magnitudes 7.0 and 5.0 at different frequencies.

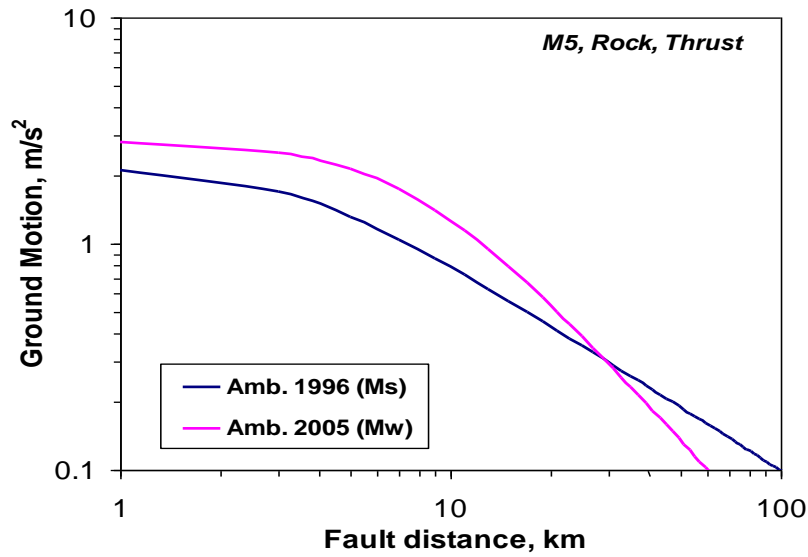


Figure 7.1. Comparison of predicted PGA using the empirical ground motion prediction equations by Ambraseys *et al.* (1996) and Ambraseys *et al.* (2005) for magnitude M 5.0.

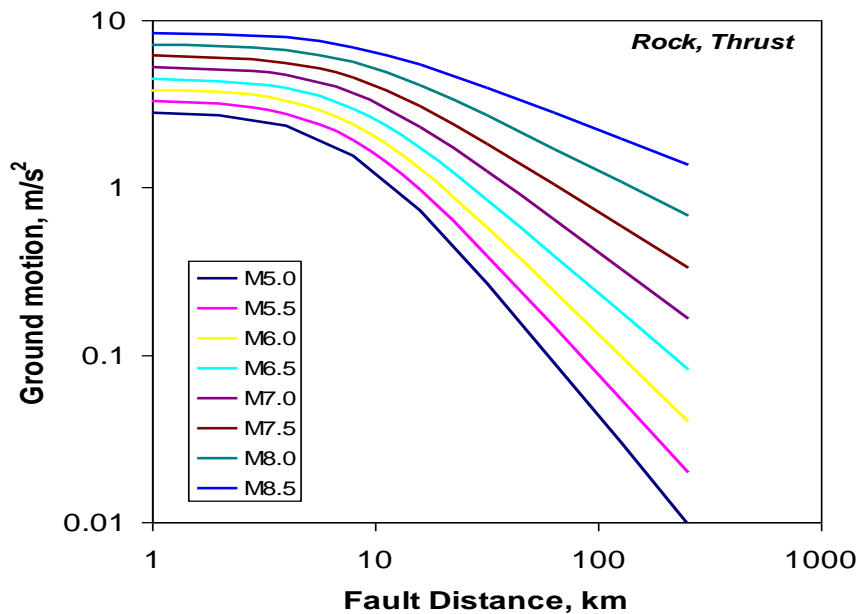


Figure 7.2. PGA predictions for a suite of magnitudes for Ambraseys *et al.* (2005).

The Ambraseys *et al.* (1996) relation was developed for Ms while the Ambraseys *et al.* (2005) was developed for Mw, partly on the same data. Fig. 7.1 compares the two relations for a magnitude 5 event, while Fig. 7.2 shows predicted PGA for a suite of magnitudes. In Fig. 7.3 the predicted spectral acceleration is plotted for two distances and magnitudes.

Ambraseys *et al.* (2005) in particular analyzed the scatter in the data relative to the predictions, and could state that they along with other authors found an increasing scatter

with decreasing magnitude as also shown in Fig. 7.3, which shows that a sigma value around 0.3 is adequate.

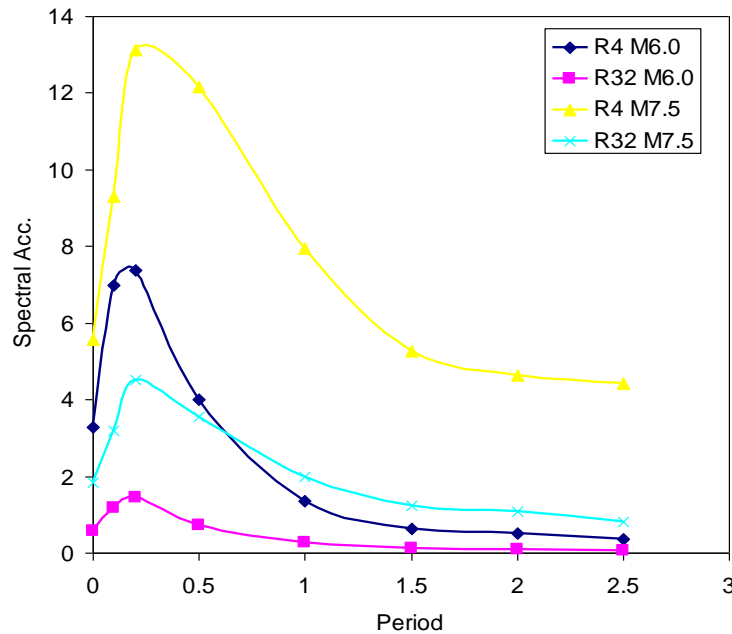


Figure 7.3. Spectral acceleration predictions for two magnitudes (6.0 and 7.5) and two distances (4 and 32 km) from Ambraseys *et al.* (2005).

In conclusion it was decided to use the Ambraseys *et al.* (2005) relation for ground motion modelling in the present study. It is furthermore based on shallow data which we know are the potentially destructive earthquakes. Finally, it is established through a rigorous quality checking that also lends trust to the results.

The  $\sigma$ -values found by Ambraseys for the various frequencies have been applied in the hazard computation model.

### 7.2.1 Sigma ( $\sigma$ ) values

The sigma values were based on Ambraseys *et al.* (2005) and are converted to CRISIS by following the relation:  $\sigma = \sigma_1 \cdot \ln(10)$

The standard deviation  $\sigma$  for such frequencies were used as:

**Table 7.1:** Sigma values for magnitude 6.5Mw based on Ambraseys *et al.* (2005)

PGA	0.1	0.2	0.5	1.0	1.5	2.0	2.5
0.58726	0.629842	0.63653	0.687082	0.754557	0.719097	0.71889	0.728077

## 8 The computational model

The target area was defined on a fine grid covering the city with spacing 0.02 degrees (approximately 2 km).

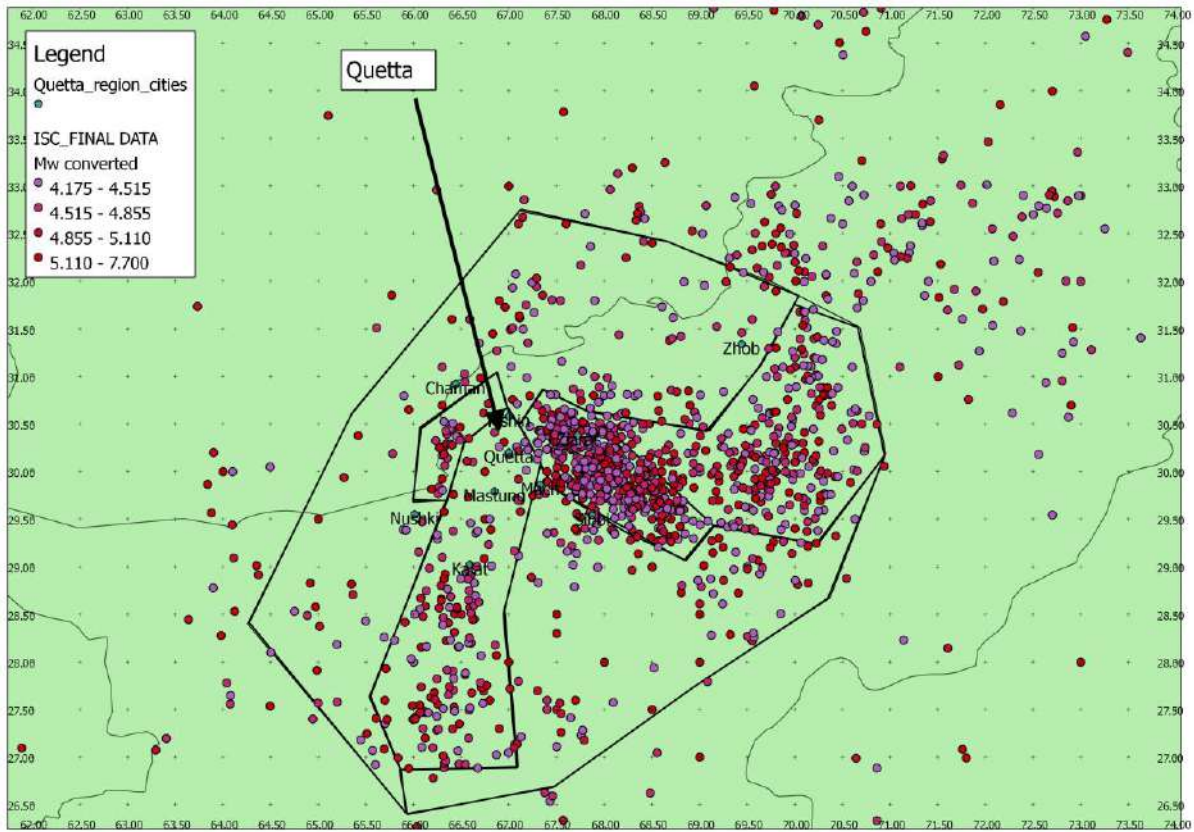


Figure 8.1. The area zones used in the model.

Table 8.1: Annual recurrence for  $M=5$  for 6 area zones used in the computational model together with mean  $M_{max}$  value (7.9).

Zone	Annual N ( $M=5$ )	$M_{max}$
Main zone (Suleiman Range)	2.43	7.9
West zone (west of Quetta)	0.84	7.9
North zone (northern Suleiman)	0.57	7.9
South zone (stretching south from Quetta)	0.92	7.9
Remain east (southeastern part)	0.612	7.9
Remain west (northwestern part)	0.934	7.9

The Table-8.1 shows the annual rates used in the computational model together with the  $b=1.14$  as derived from the overall data. Furthermore  $M_{max}$  of 7.9 was used. This is regarded as the maximum credible earthquake that may take place in the region albeit tapered off against  $M8.1$ .

For the area sources the Gutenberg-Richter relations were used as basis for modeling the seismic activity. The fault sources were modelled as an added contribution. This attempts to cover the possibly higher seismicity than observed in the short observation period. The

cumulative moment release of the modeled faults lines amount to less than 10% of the cumulative moment release of the area sources. The faults (structures) are modeled as Gutenberg-Richter distributions with  $M=7.3$  as the minimum magnitude and 7.9 as the maximum magnitude.

The maximum contribution distance was set to 256 km.

Hazard was computed for 8 periods and for 20 ground motion levels ranging from 0.01 to 20  $m/s^2$ .

## 9 Seismic hazard and loading results

The hazard results obtained for the central part of Quetta city is seen in Fig. 9.1. There is a variation within Quetta city, however, the PGA for 500 years return period averages to 4.72  $m/s^2$ . This corresponds to rock outcrop values.

The values obtained are characterized as very high, but may indeed confirm the damages from previous earthquakes as e.g. the 1935 earthquake. It is noted that the values presented below are for rock sites. The spectra will be modified by local soil conditions.

*Table 9.1. Ground motion results for three return periods and 8 periods for central Quetta at rock site.*

Period (seconds)	Horizontal Ground Motion ( $m/s^2$ ) for recurrence period 100 years	Horizontal Ground Motion ( $m/s^2$ ) for recurrence period 500 years	Horizontal Ground Motion ( $m/s^2$ ) for recurrence period 1000 years
PGA	2.35	4.79	6.15
0.10	5.07	10.33	13.19
0.20	5.79	11.56	14.78
0.50	3.36	7.73	10.81
1.00	1.47	4.07	6.28
1.50	0.81	2.42	3.86
2.00	0.69	2.11	3.39
2.50	0.49	1.64	2.83

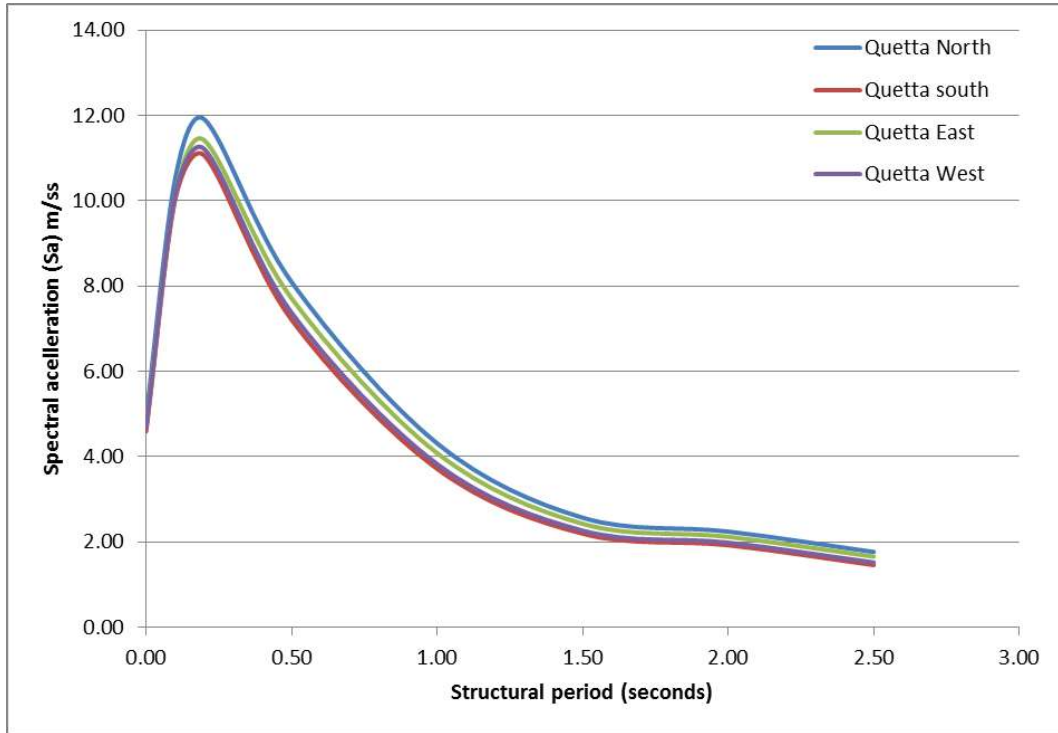


Figure 9.1. Results for Quetta for rock sites. Values are for the  $0.002 \cdot 10^{-4}$  annual exceedance rate (500 years recurrence). While there are differences, the PGA averages to 4.72  $m/s^2$  for this return period.

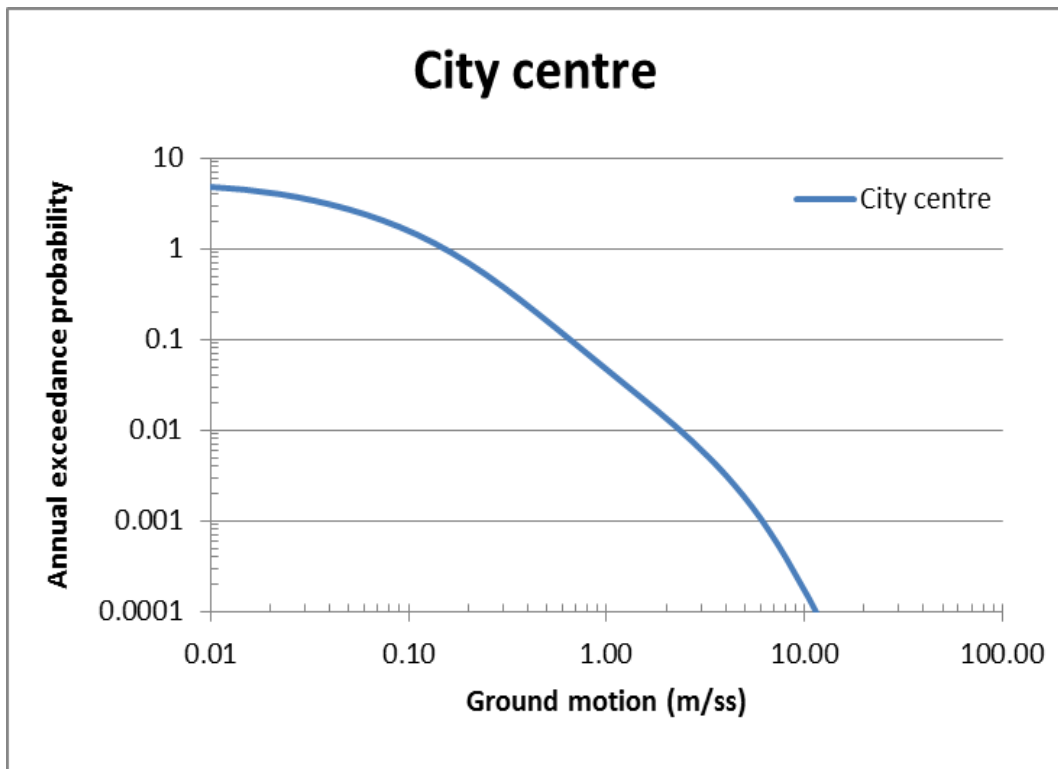


Figure 9.2. Hazard curve for central Quetta for rock sites.

## 10 References

- Abrahamson N. and J. Bommer (2005). Probability and uncertainty in seismic hazard analysis. *Earthq. Spectr.*, 21, 603-607.
- Aitchison, J.C., Ali, J.R. and Davis, A.M. (2007): When and where did India and Asia collide? *Journal of Geophysical Research, Solid Earth* 112: B05423, doi:10.1029/2006JB004706
- Akkar, S. and J.J. Bommer (2006): Empirical prediction equations for peak ground velocity derived from strong motion records from Europe and Middle East. *Bull. Seism. Soc. Am.* 97(2), 511–530.
- Akkar, S. and J.J. Bommer (2007): Prediction of Elastic Displacement Response Spectra in Europe and the Middle East. *Earthq. Eng. Struct. Dyn.*
- Akkar, S. and J.J. Bommer (2007): Prediction of Elastic Displacement Response Spectra in Europe and the Middle East. *Earthq. Eng. Struct. Dyn.*, in press.
- Ambraseys N. and R. Bilham (2003): Earthquakes and associated deformation in norther Baluchistan 1892-2001. *Bull. Seism. Soc. Am.*, 93, 4, pp. 1573-1605.
- Ambraseys, N.N., J. Douglas, S.K. Sarma, and P.M. Smit. (2005): Equations for the Estimation of Strong Ground Motions from Shallow Crustal Earthquakes Using Data from Europe and the Middle East: Horizontal Peak Ground Acceleration and Spectral Acceleration. *Bulletin of Earthquake Engineering* 3, 1–53.
- Ambraseys, N.N., K.A. Simpson, and J.J. Bommer (1996): Prediction of horizontal response spectra in Europe. *Earth. Eng. Struct. Dyn.* 25, 371–400.
- Atkinson, G.M. and D.M. Boore (1995): Ground-motion relations for Eastern North America. *Bull. Seism. Soc. Am.* 85, 17–30.
- Bachman R. E. and D. R. Bonneville (2000): The Seismic Provisions of the 1997 Uniform Building Code. *Earthquake Spectra* 16, pp. 85-100 (2000); doi:10.1193/1.1586084
- Boore, D.M., W.B. Joyner, and T.E. Fumal (1997): Equations for estimating horizontal response spectra and peak accelerations from western North American earthquakes: A summary of recent work. *Seism. Res. Lett.* 68, 128–153.
- Building Codes Of Pakistan Seismic Provisions (2007): Government of Islamic republic of Pakistan Ministry of Housing and Works, Islamabad.
- Caillot, V. and P.-Y. Bard (1993): Magnitude, distance and site dependent spectra from Italian accelerometric data. *Europ. Earthq. Eng.* 1, 37–48.
- Cornell, C.A. (1968): Engineering seismic risk analysis. *Bull. Seism. Soc. Am.* 58, 1583–1606.
- Das Aaroon Joshua (2011): Vulnerability assessment of structures subjected to earthquakes (VASE) in Pakistan thesis for the Master of Science at National Institute of Transportation, School of Civil and Environmental Engineering, NUST, Islamabad, Pakistan.
- Der Kiureghian, A. and A.H.-S. Ang (1977): A fault rupture model for seismic risk analysis. *Bull. Seism. Soc. Am.* 67, 1173–1194.
- Din Muhammad (2008): Earthquake risks in Quetta and surrounding regions, Balochistan, Pakistan. 33'd International Geology Congress, Oslo, August, 2008.

Global CMT Catalogue Search: available at web page:  
<http://www.globalcmt.org/CMTsearch.html>

Griesbach, C.L., (1893): Notes on the earthquake in Baluchistan on the 20th December 1892: Records Geol. Survey India, v.26, p.57-64.

Khan, M. A., Javed, M. Waqas, Sayab, M. (2012): Fault Map and Associated Database of Fault Parameters for Pakistan. Earthquake Model of Middle East (EMME) International Project-WP1 Report (in Press).

Lawrence R. D. and S. Yeasts (1979): Geological reconnaissance of the Chaman fault in Pakistan. Geodynamics of Pakistan. pp. 351-357.

McGuire, R.K. (1976): FORTRAN computer programs for seismic risk analysis. U.S. Geol. Survey Open-File Report No 76-67.

McGuire, R.K. (1978): FRISK: Computer program for seismic risk analysis using faults as earthquake sources. U.S. Geol. Survey Open File-Report No 78-1007.

Mortgat, C.P. and H.C. Shah (1979): A Bayesian model for seismic hazard mapping. Bull. Seism. Soc. Am. 69, 1237–1251.

Niamatullah M, Durrani K H, Qureshi A R, Khan Z, Kakar D M, Jan M R, Ghaffar A 1989 Emplacement of Bibai and Gogai Nappes, NE of Quetta Geol. Bull., Univ. of Peshawar, vol. 22, pp153-158.

NORSAR and Risk Engineering, Inc. (1991): Ground motions from earthquakes on the Norwegian Continental Shelf. Report for Operatørkomite Nord (OKN), Stavanger, Norway.

Ordaz, M., A. Aguilar, and J. Arboleda (2003): Crisis 2003. Program for computing seismic Hazard, Ver. 3.01.

Pinhey, L. A. (1938): the Quetta earthquake of 31 May 1935, Govt of India, New Delhi.

Powell. C. McA, (1979): A Speculative tectonic history of Pakistan and surroundings Geodynamis of Pakistan. Geological survey of Pakistan, Quetta.

Rafi Z., N. Ahmed, S. Ur Rehman, T. Azeem and Abd el-Aziz K.A. (2011): Analysis of the Quetta-Ziarat Earthquake of 29 October 2008 in Pakistan. Arab J. GeoSci, pp. 1-7, DOI:10.1007/s12517-011-0485-2.

Reiter L. (1990) Earthquake Hazard Analysis; Issues and Insights. Columbia University Press.

Sarwar G, Dejong K A (1979): Arcs, oroclines, syntaxes: the curvature of mountain belts in Pakistan. Geodynamics of Pakistan p.341-350.

Scordilis, E.M. (2006): Empirical Global Relations Converting Ms and mb to Moment Magnitude. Journal of Seismology; 10, pp. 225-236.

Seismic Hazard Analysis and Zonation for Pakistan, Azad Jammu and Kashmir (2007): Report by Pakistan Meteorological Department and NORSAR.

Seismological Society of America, v. 84, p. 974-1002.

Stepp, J.C. (1972): Analysis of completeness of the earthquake sample in the Puget Sound area and its effect on statistical estimates of earthquake hazard, in Proceedings First

Szeliga W., D. Schelling and R. Bilham (2009): Listric earthquake faulting and triggering in the Mach/Shiragh/Quetta earthquakes. Science Rendezvous Posters; <http://cires.colorado.edu/events/rendezvous/2008/posters/szeliga.html>

Szeliga, W., S.E. Hough, S. Martin, and R. Bilham (2009): Intensity, magnitude, location and attenuation in India for felt earthquakes since 1762, *Bull Seism, Soc. Am.*

Toro, G.R., N.A. Abrahamson, and J.F. Schneider (1997): Model of strong ground motions from earthquakes in Central and Eastern North America: Best estimates and uncertainties. *Seism. Res. Lett.* 68, 41–57.

US Army Corps of Engineers (1984): *SEISMIC DESIGN FOR BUILDINGS*. TI 809-04 31 December 1998

Wells, D.L., and Coppersmith, K.J. (1994): New empirical relationships among magnitude, rupture length, rupture width, and surface displacements. *Bulletin of the*

West, W.D. (1934): The Baluchistan earthquake of of 25th and 27th Aug 1931, *Mem. Geol. Surv. India* 67, p. 01-82.

West, W.D. (1937): Earthquakes in India, *Proc. Indian Sci., Congress, Delhi*, Vol. 24, 189-224

Youngs, R.R. and K. Coppersmith (1985): Implications of fault slip rates and earthquake recurrence models to probabilistic seismic hazard estimates. *Bull. Seism. Soc. Am.* 75, 939–964.

## 11 Glossary

**Accelerogram** - Time history of accelerations.

**Active fault** - (1) A fault that has had sufficiently recent displacements so that, in the opinion of the user of the term, further displacements in the foreseeable future are considered likely. (2) A fault that on the basis of historical, seismological, or geological evidence has a high probability of producing an earthquake. (3) A fault that may produce an earthquake within a specified exposure time, given the assumptions adopted for a specific seismic-risk analysis.

**Attenuation** - The reduction in amplitude of a wave with time or distance travelled, most often used for the decrease in amplitude of ground motion with increase in distance from the source. This attenuation is due to two mechanisms, one is the distribution of energy over a larger volume as the distance increases, the other is the loss of energy due to internal damping. The latter effect is frequency dependent and gives higher attenuation of the high frequency motion.

**Attenuation law** - A description of the behaviour of a characteristic of earthquake ground motion as a function of the distance from the source of energy.

**b-value** - A parameter indicating the relative frequency of earthquakes of different sizes. It is the slope of a straight line indicating absolute or relative frequency (plotted logarithmically) versus earthquake magnitude (or meizoseismal intensity), often shown to be stable over a wide range of magnitudes. The B-value indicates the slope of the curve of the Gutenberg-Richter recurrence relationship.

**Body waves** - A seismic wave that travels through the interior of an elastic material. These waves consist of compressional waves (P-waves) and shear waves (S-waves). Near the source most of the energy carried is in the form of body waves.

**Capable fault** - A fault along which it is mechanically feasible for sudden slip to occur. Evaluation of capability is based on geologic and/or seismic evidence. Capable is used for faults where it is possible, but not certain, that earthquakes can occur, often used synonymously with potentially active faults.

**Continental plate** - A large rigid part of the earth's crust and upper mantle (lithosphere) which moves relative to the other continental plates. The speed of movement may be up to 15-20 cm/year. Scandinavia belongs to the Eurasian continental plate.

**Crust** - The outer major layer of the earth, separated from the underlying mantle by the Moho discontinuity, and characterized by P-wave velocity less than 8 km/s. The thickness of the crust in the Norwegian Continental Shelf in the range 15-25 km.

**Damping** - Loss of energy in wave motion due to transfer into heat by frictional forces. In engineering often expressed relative to the critical damping,  $C_{cr} = 2(KM)^{1/2}$ , where K and M are stiffness and mass of the vibrating system, respectively.

**Design acceleration** - A specification of the ground acceleration at a site in terms of a single value such as the peak or rms; used for the earthquake-resistant design of a structure (or as a base for deriving a design spectrum). See *Design time history*.

**Design earthquake** - (1) A specification of a seismic ground motion at a site; used for the earthquake-resistant design of a structure. (2) An earthquake event used the earthquake-

resistant design of structures, which may or may not be equivalent to the maximum earthquake prescribed for the installation.

**Design event (Design seismic event)** - A specification of one or more earthquake source parameters, and of the location of energy release with respect to the site of interest; used for the earthquake-resistant design of structures.

**Design ground motion** - Description of ground shaking (e.g., time history, response spectrum) at a given site used for the earthquake-resistant design of structures; in modern hazard studies usually the result of contributions from all seismic sources surrounding the site and not corresponding to any specific design earthquake. See *Design earthquake*.

**Design spectrum** - A set of curves for design purposes that gives acceleration, velocity or displacement (usually absolute acceleration, relative velocity, and relative displacement of the vibrating mass) as a function of period of vibration and damping.

**Deterministic hazard assessment** - An assessment that specifies single-valued parameters such as maximum earthquake magnitude or peak ground acceleration without consideration of likelihood.

**Duration** - A qualitative or quantitative description of the length of time during which ground motion at a site shows certain characteristics (perceptibility, violent shaking, etc.).

**Earthquake** - A sudden motion or vibration in the earth caused by the abrupt release of energy in the earth's lithosphere; shaking of the ground by different types of waves generated by tectonic movements or volcanic activity. By far the largest number of destructive earthquakes are caused by tectonic movements. An earthquake is initiated when the accumulated tectonic stresses at any one point in the ground become greater than the strength at this point. Release of stress at one point may increase the stresses nearby, and result in a progressive rupture which may propagate for several hundred kilometres. The rupture will almost invariably occur along old zones of weakness (faults), and the wave motion may range from violent at some locations to imperceptible at others.

**Earthquake cycle** - For a particular fault, fault segment, or region, a period of time that encompasses an episode of strain accumulation and its subsequent seismic relief.

**Epicentre** - The point on the earth's surface that is directly above the focus (hypocenter) of an earthquake.

**Equal hazard spectrum** - Specifies ground motion (usually pseudo-relative velocity) as a function of natural period and damping level for a given probability of occurrence. The term is sometimes used synonymously with design spectrum or response spectrum.

**Deterministic hazard assessment** - An assessment that specifies single-valued parameters such as maximum earthquake magnitude or peak ground acceleration without consideration of likelihood.

**Fault** - A fracture or a zone of fractures along which displacement has occurred parallel to the fracture. Earthquakes are caused by a sudden rupture along a fault or fault system; the ruptured area may be up to several thousand square kilometres. Relative movements across a fault may typically be tens of centimetres for magnitude 6.0-6.5 earthquakes, several meters for magnitude 7-8 earthquakes.

**Fault slip rate** - The rate of slip on a fault averaged over a time period involving several large earthquakes. The term does not necessarily imply fault creep.

**Geologic hazard** – A geologic process (e.g., land sliding, soil liquefaction, active faulting) that during an earthquake or other natural events may produce adverse effects on structures.

**Hypocenter** - The point where the earthquake started, also called focus. Hypocenter depths are typically 30 km and less for shallow earthquakes, several hundreds of kilometres for earthquakes occurring in subduction zones. Most earthquakes in Fennoscandia originate at depths between 10 and 30 km.

**Intensity (of an earthquake)** - A qualitative or quantitative measure of the severity of ground shaking at a given site (e.g., MSK intensity, Modified Mercalli intensity, Rossi-Forel intensity, Housner Spectral intensity, Arias intensity, peak acceleration, etc.) based on effects of the earthquake such as how the earthquake was felt, damage to structures, how people reacted, soil or rock slides, etc.

**Interplate earthquake** - An earthquake along a tectonic plate boundary. Most earthquakes are caused by the relative plate movements along plate margins, i.e., between plates.

**Intraplate earthquake** - An earthquake within a tectonic plate. Scandinavia belongs to the Eurasian plate and is well removed from the nearest plate boundary.

**Isoseismal** - Contour lines drawn to separate one level of seismic intensity from another.

**Logic tree** - A formalized decision flow path in which decisions are made sequentially at a series of *nodes*, each of which generates *branches* flowing to subsequent nodes.

**Macroseismic** - Ground shaking which gives noticeable effects. See *Intensity*.

**Magnitude** - A measure of earthquake size at its source. Magnitude was defined by C. Richter in 1935 as: “The logarithm to the trace amplitude in 0.001 mm on a standard Wood-Anderson seismometer located 100 km from the epicentre” The Wood-Anderson instrument measures the responses in the period range near 1 sec. Other magnitude scales have later been devised based on the responses measured in other period ranges, and on maximum amplitudes of specific wave forms Some of the more commonly used magnitude scales are:

1.  $M_L$  = local magnitude, similar to the original Richter magnitude. Usually determined from shear wave response in the period range near 1 sec. at relatively close distances from the epicentre (< 600 km).
2.  $m_b$  = body wave magnitude is based on the largest amplitude of body waves, usually the compressional component with period near 1 sec.
3.  $M_s$  = surface wave magnitude is measured in the period range near 20 sec.
4.  $M_w$  = moment magnitude is based on the seismic moment and be computed directly from source parameters or from long period components in the earthquake record. Symbol  $M$  is also used for this magnitude.

Magnitude scales are also based on other earthquake parameters such as felt area, length of rupture and surface displacement, and area within different intensity zones.

A large number of empiric relations between magnitude and other earthquake parameters such as energy, fault movement, fault area, intensity, maximum acceleration, etc., are available. Such relations may differ considerably from one seismic region to another.

**Maximum credible, expectable, expected, probable** - These terms are used to specify the largest value of a variable, for example, the magnitude of an earthquake that might reasonable be expected to occur. In the view of the Earthquake Engineering Research Institute, U.S (EERI) Committee on Seismic Risk (cf. *Earthquake Spectra*, Vol. 1, pp. 33-40), these are misleading terms and their use is discouraged.

**Maximum credible earthquake** - The maximum earthquake that is capable of occurring in a given area or on a given fault during the current tectonic regime; the largest earthquake that can be reasonably expected to occur (USGS); the earthquake that would cause the most severe vibratory ground motion capable of being at the site under the current known tectonic framework (US Bureau of Reclamation). "Credibility" is in the eyes of the user of the term.

**Maximum earthquake** - The maximum earthquake that is thought, in the judgment of the user, to be appropriate for consideration in the location and design of a specific facility.

**Maximum possible** - The largest value possible for a variable. This follows from an explicit assumption that larger values are not possible, or implicitly from assumptions that related variables or functions are limited in range. The maximum possible value may be expressed deterministically or probabilistically.

**Maximum probable earthquake** - The maximum earthquake that, in the judgment of the user, is likely to occur in a given area or on a given fault during a specific time period in the future.

**Mean (average) recurrence interval** - The mean (average) time between earthquakes or faulting events with specific characteristics (e.g., magnitude  $\geq 5$ ) in a specified region or in a specific fault zone.

**Mean (average) return period** - The mean (average) time between occurrences of ground motion with specified characteristics (e.g., peak horizontal acceleration  $>0.1$  g) at a site. Equal to the inverse of the annual probability of exceedance.

**Moho** - Mohorovicic discontinuity, a sharp discontinuity in seismic velocities separating the earth's crust from the underlying mantle, also called the crust-mantle boundary. P wave speeds are typically 6.7-7.2 km/s in the lower crust and 7.6-8.6 km/s at the top of the upper mantle.

**Neotectonics** - (1) The study of post-Miocene structures and structural history of the earth's crust. (2) The study of recent deformation of the crust, generally Neogene (post-Oligocene). (3) Tectonic processes now active, taken over the geologic time span during which they have been acting in the presently observed sense, and the resulting structures.

**P wave** - A seismic body wave with particle motion in the direction of propagation, also called compressional wave even though the motion alternates between extension and compressions.

**Potentially active fault** - A term used by different people in different ways, but sometimes referring to a fault that has had displacements on it within the late Quaternary period.

**Pseudo acceleration (PSA)** - See Response spectrum.

**Pseudo velocity (PSV)** - See Response spectrum.

**Response spectrum** - Describe the maximum response of single-degree-of-freedom systems (linear oscillator) to given ground motions (e.g., an earthquake accelerogram) as a function of the period and the damping of the system. The responses may be pseudo acceleration, pseudo velocity or relative displacement. Pseudo acceleration and pseudo velocity values may be expressed in an approximate way from the relative displacement through the relation: where  $PSA/\omega^2 = (PSV)/\omega = RD$  is pseudo acceleration, PSV is pseudo velocity and RD relative displacement, respectively, and  $\omega$  is circular frequency. By using the pseudo values, all three responses can be plotted together in a logarithmic, tripartite nomogram.

**Return period** - Same as recurrence interval, average time period between earthquakes of a given size in a particular region, cycle time.

**S wave** - A seismic body wave with particle motion perpendicular to the direction of propagation, also called shear wave. The passage of an S-wave involves a pure shear of the medium.

**Secondary effects** - Nontectonic surface processes that are directly related to earthquake shaking or to tsunamis.

**Seismic activity rate** - The mean number per unit time of earthquakes with specific characteristics (e.g., magnitude  $\geq 5$ ) originating on a selected fault or in a selected area.

**Seismic design load effects** - The actions (axial forces, shears, or bending moments) and deformations induced in a structural system due to a specified representation (time history, response spectrum, or base shear) of seismic design motion.

**Seismic design loading** - The prescribed representation (time history, response spectrum, or equivalent static base shear) of seismic ground motion to be used for the design of a structure.

**Seismic event** - The abrupt release of energy in the earth's lithosphere, causing an earthquake.

**Seismic hazard** - Any physical phenomenon or effect (e.g., ground shaking, ground failure, landsliding, liquefaction) associated with an earthquake that may produce adverse effects on human activities, representing the earthquake's potential danger. Specifically, the probability of occurrence over a given time period in a given location of an earthquake with a given level of severity. Seismic exposure may be used synonymously with seismic hazard.

**Seismic moment** - The area of a fault rupture multiplied by the average slip over the rupture area and multiplied by the shear modulus (rigidity) of the affected rocks. Seismic moment can be determined directly from the long period asymptote of path corrected far field displacement spectra. Dimension dyne-cm or N-m.

**Seismic moment rate** - The long term rate at which seismic moment is being generated.

**Seismic risk** - The probability that social or economic consequences of earthquakes will equal or exceed specified values at a site, at several sites, or in an area, during a specified exposure time; the likelihood of human and property loss that can result from the hazards of an earthquake. Often expressed as hazard times vulnerability.

**Seismic zone** - A generally large area within which seismic design requirements for structures are constant. Some times used synonymously with *Seismogenic zone*.

**Seismic zoning (zonation)** - The process of determining seismic hazard at many sites for the purpose of delineating seismic zones. Some times used synonymously with *Seismotectonic zoning*.

**Seismicity** - The occurrence of earthquakes in space and time.

**Seismogenic structure** - A geologic structure that is capable of producing an earthquake.

**Seismogenic zone (province)** - A planar representation of a three-dimensional domain in the earth's lithosphere in which earthquakes are inferred to be of similar tectonic origin; may also represent a fault. See *Seismotectonic zone*.

**Seismotectonic zone (province)** - A seismogenic zone in which the tectonic processes causing earthquakes have been reasonably well identified; usually these zones are fault zones. In seismic hazard analyses often used to describe a region (area) within which the active geologic and seismic processes are considered to be relatively uniform.

**Seismotectonic** - The study of the tectonic component represented by seismic activity a subfield of active tectonics concentrating on the seismicity, both instrumental and historical, and dealing with geological and other geophysical aspects of seismicity.

**Strain** - Change in the shape or volume of a body as a result of stress.

**Stress** - Force per unit area.

**Stress drop** - The sudden reduction in stress across the fault plane during rupture. Intraplate earthquakes have in general higher stress drop than interpolate earthquakes. Typical values are 1-10 MPa (10-100 bars).

**Surface waves** - Seismic waves travelling along the surface of the earth or along layers in the earth's crust, with a speed less than that of S waves. The two most common types are Raleigh waves and Love waves.

**Tectonics** - A branch of geology dealing with the broad architecture of the outer part of the earth, that is, the regional assembling of structural or deformational features, a study of their mutual relations, origin, and historical evolution.

**Vulnerability** - (1) The degree of loss to a given element at risk, or set of such elements, resulting from an earthquake of a given magnitude or intensity, usually expressed on a scale from 0 (no loss) to 10 (total loss). (2) Degree of damage caused by various levels of loading. The vulnerability may be calculated in a probabilistic or deterministic way for a single structure or groups of structures.